How can a cause-of-death reduction be compensated for by the population heterogeneity? A dynamic approach.

Sarah Kaakai, Héloïse Labit-Hardy, Séverine Arnold (-Gaille), Nicole Karoui

How can a cause-of-death reduction be compensated for by the population heterogeneity? A dynamic approach.

Sarah Kaakai[1], Héloïse Labit Hardy[2], Séverine Arnold (-Gaille)[3],
Nicole El Karoui[4]

April 11, 2019

Abstract

A growing number of studies indicate a widening of socioeconomic inequalities in mortality over the past decades. It has therefore become crucially important to understand the impact of heterogeneity and its evolution on the future mortality of heterogeneous populations. In particular, recent developments in multi-population mortality have raised a number of questions, among which is the issue of evaluating cause-of-death reduction targets set by national and international institutions in the presence of heterogeneity.

The aim of this paper is to show how the study of the population data and the population dynamics framework contribute to addressing these issues, by providing a new viewpoint on the evolution of aggregate mortality indicators in the presence of heterogeneity. Our findings rely on two unique datasets on the English population and cause-specific number of deaths by socioeconomic circumstances, over the period 1981-2015.

The analysis of the data first highlights the complexity of recent demographic developments, characterized by significant composition changes in the population, with considerable variations according to the age class or cohort, along with a widening of socioeconomic inequalities. We then introduce a dynamic framework for studying the impact of composition changes on the mortality of the global population. In particular, we are interested in quantifying the impacts of cause-of-death mortality reduction in comparison with changes of composition in a heterogeneous population. We show how a cause of death reduction could be compensated for in the presence of heterogeneity, which could lead to misinterpretations when assessing public policies impacts and/or for the forecasting of future trends.

JEL: G22, J11, C60

Keywords: Population Dynamics, Deprivation, Heterogeneity, Cause-of-Death Mortality, Cohort Effect

[1]Corresponding author, Risk and Insurance Institute and Laboratoire Manceau de Mathématiques, Le Mans University, 72085 Le Mans, France. Email: sarah.kaakai@univ-lemans.fr.

[2]ARC Centre of Excellence in Population Ageing Research (CEPAR), UNSW Australia, Sydney NSW 2052, Australia. Email: h.labithardy@unsw.edu.au.

[3]Département de Sciences Actuarielles (DSA), Faculté des HEC, Extranef, Université de Lausanne, 1015 Lausanne, Suisse. Email: severine.arnold@unil.ch.

[4]Laboratoire de Probabilités, Statistique et Modélisation (LPSM), Université Pierre et Marie Curie, 4 Place Jussieu, 75005 Paris, France. Email: nicole.el_karoui@upmc.fr.

1 Introduction

Large populations such as national populations usually present some heterogeneity, in the sense that individuals with different characteristics (gender, social characteristics, neighborhood, etc.) exhibit different demographic behaviors. Whenever possible, taking into account these characteristics can provide useful information, but at the same time, modeling the population in the presence of heterogeneity is much more complex.

Research on the relationship between socioeconomic status and mortality can be traced back as far as the nineteenth century (see e.g. Villermé (1830), or reports of the General Registrar Office in England). Since then, an important body of work has investigated the links between socioeconomic status (SES) or neigborhood, and mortality and causes of death (Pamuk (1985), Marmot et al. (1991), Mackenbach et al. (1997)). More recently, a growing number of studies have shown that the socioeconomic gradient in mortality is increasing in a number of countries including England (Elo (2009), National Research Council (2011), Office for National Statistics (2015b), El Karoui et al. (2018)). These gaps are even been forecast to increase further (Villegas and Haberman (2014)).

The widening of these socioeconomic gaps has led a number of pension funds and insurance companies to rethink their models in order to tackle this heterogeneity issue and to understand the potential impact of socioeconomic inequalities. For instance, the Life & Longevity Markets Association (LLMA) and the Institute and Faculty of Actuaries (IFoA) have recently commissioned a series of reports on longevity basis risk (Haberman et al. (2014), Li et al. (2017)). Indeed, not taking into account socioeconomic differences can have substantial impacts for insurance companies or governments, by leading, for instance, to errors in funding of annuity and pension obligations (see e.g. Meyricke and Sherris (2013); Villegas and Haberman (2014)) or increasing the basis risk. Consequently, a growing literature, facilitated by the recent release of data at a finer level, has recently taken an interest in the joint modeling and forecasting of the mortality of socioeconomic subgroups (Jarner and Kryger (2011); Villegas and Haberman (2014); Li et al. (2015); Cairns et al. (2016)). However, there are still many open questions regarding the impact of heterogeneity on mortality modeling. The classical approach developed in actuarial science focuses on mortality data only, but the information contained in the population age-structure is crucial in order to understand the effects of heterogeneity on aggregate mortality trends. Thus, we argue in this paper that, in order to address these questions, it is necessary to consider the population evolution over time: namely, the population dynamics.

The population heterogeneity also raises issues concerning the evaluation of public health policies. Indeed, a number of institutions have defined public health goals in terms of cause-of-death mortality reduction (Department of Health (2003), World Health Organization (2013)). However, at the national level, the interpretation of standard indicators such as the period life expectancy can be complex in the presence of heterogeneity, since individuals with different socioeconomic status are affected differently by diseases (Bajekal et al. (2013b), National Research Council (2011), Villegas (2015)). For instance, by studying recommendations from the World Health Organization, Alai et al. (2017)

have shown that these recommendations could actually increase life expectancy gaps in England, despite an increase of the national life expectancy. More generally, it is difficult to evaluate if changes in cause-of-death mortality have occurred by only analyzing data aggregated at the national level, since the population age-structure and socioeconomic composition change at the same time.

The aim of this paper is to show how the study of the population data and the population dynamics framework shed new light on the evolution of aggregate mortality patterns and longevity indicators in the presence of heterogeneity.

Our first goal is not to provide a new multi-population or cause-of-death mortality model, but rather to use the population dynamics point of view in order to represent the data differently than what is usually done. The study is based on two datasets obtained from the UK Office for National Statistics (ONS) and the Department of Applied Health Research (DAHR), University College London[1], containing data on the English population and cause-specific number of deaths by age, gender and socioeconomic circumstance over the period 1981-2015. Our analysis reveals significant variations of the population's socioeconomic composition, across the different age classes and over time. This heterogeneity is combined with an increase in mortality differences, confirming observations of Lu et al. (2014) and Villegas and Haberman (2014) over the period 1981-2007, which magnifies the impact of population composition changes on aggregated mortality. Our second goal is to provide a *dynamic* framework in order to study these composition changes and their effect on aggregated mortality over time. In particular, we are interested in studying cause-of-death mortality reduction in the presence of heterogeneity. In the demographic literature, Shkolnikov et al. (2006) and Jasilionis et al. (2011) have studied the contribution of compositional changes to mortality evolution, but rather with a static approach based on decomposition methods. By introducing an heterogeneous McKendrick-Von Foerster population dynamics model, we adopt a dynamic approach to test the impact of cause-of-death mortality reduction under different demographic scenarios. The framework used in this study is not aimed at being a predictive tool, but rather a tool for experimenting and simulating different scenarios. This framework allows us to isolate demographic changes of different natures (cause-of-death reduction, adverse compositional changes) and to quantify how they interact when they are combined. In particular, we show that the reduction of a cause of death may not necessarily result in an improvement in aggregate mortality rates or life expectancy, if the composition of the population changes at the same time. Thus, the effect of public health policies could be misinterpreted if only aggregated data are studied.

The remainder of this paper is organized as follows. In Section 2, we introduce the data used to carry out our study. Particular emphasis is being placed on presenting the main features of the age structures of the subpopulations grouped by socioeconmic circumstances, and their evolution over time. In Section 3, we present the deterministic population dynamics model used in Section 4. Section 4 presents our numerical results. We first show how different socioeconomic composition of the age classes can impact

[1]The authors thank Madhavi Bejekal, Senior Research Fellow at the Department of Applied Health Research (DAHR), University College London, for her assistance in obtaining the dataset from the DAHR.

the life expectancy and mortality improvement rates. Then, we show how a cause of death reduction could be compensated for by adverse compositional changes, induced by heterogeneity in fertility rates.

2 What can be learned from the data

In this section, we present the two datasets used in this paper. Particular emphasis is made on the evolution of the age structure of the subpopulations grouped by deprivation level, which we consider to be an important contribution of the study.

2.1 Datasets

The data we use provide mid-year population estimates in England by age class and socioeconomic circumstances for the years 1981-2015, combined with the number of deaths by age, cause and socioeconomic circumstance. Our study is based on two data sources:
(i) The first dataset was provided to us by the Department of Applied Health Research (DAHR) at University College London in the UK, and is based on the Index of Multiple Deprivation 2007 (IMD 2007) for the 1981-2006 period.
(ii) The second dataset was released in 2017 by the Office for National Statistics (ONS)[2], and is based on the IMD 2015 for the 2001-2015 period.

Deprivation Criterion In both datasets, socioeconomic circumstances are measured by the Index of Multiple Deprivation (IMD). The IMD is a geographically based index, created in order to provide an official measure of multiple deprivation dimensions at the level of small areas called LSOAs[3], each composed of about 1500 individuals (see Noble et al. (2007) and Department for Communities and Local Government (2015) for more details). The IMD is based on the measure of seven broad socioeconomic factors: income, employment, health, education, barriers to housing and services, living environment and crime. The IMD score of a LSOA is used as a SES proxy for individuals living in the small area. The index also includes information on the physical and social environment of individuals (by including, for instance, the road distance to a GP surgery and supermarket, or crime statistics), which can have a significant influence on health outcomes (Diez Roux and Mair (2010); Nandi and Kawachi (2011)).
One limitation of using area-based measurements is that they apply the same level of deprivation to all individuals living in an area. However, LSOAs are rather small areas and geographical data are often more available on a large scale than multiple individual socioeconomic measurements. We also note that the IMD is computed at fixed dates, while being applied to a longer time period (e.g. IMD 2007 applied to the period 1981-2007). The implications of using a fixed IMD quintile allocation have been discussed comprehensively in Bajekal et al. (2013a) and in Appendix D of Lu et al. (2014), based

[2]Publicly available on the ONS website (www.ons.gov.uk) under the reference number 006925.

[3]In 2007, there were 32,482 Lower Layer Super Outupt areas (LSOAs) in England (34,753 in 2011) (Office for National Statistics (2012)).

on the period 1981-2001. Our comparison of data computed with the IMD 2007 and IMD 2015 for the overlapping period 2001-2006 also gives very similar results. See Appendix A for a more detailed discussion on this issue.

Structure of data Our two data sources are based on a *relative* measurement of deprivation. LSOAs are ranked by their IMD scores and grouped into five deprivation quintiles numbered from 1 to 5: IMD quintile 1 (IMD Q1) for the least deprived quintile, to IMD quintile 5 (IMD Q5) for the most deprived quintile. It is worth noting that for each year, the five deprivation quintiles based on the LSOAs' ranking comprise approximately the same number of individuals. Specific features of each datasets are summarized in Table 1 and 2[4].

	Dataset 1	Dataset 2
Deprivation index	IMD 2007	IMD 2015
Time period	1981-2006	2001-2015
Ages	25-85+	0-90+
Population age group	5 years	1 year
Deaths age group	5 years	1 year 5 years per cause

Table 1: Datasets

	Datasets	
	1	2
Cardiovascular diseases	×	×
Neoplasms	×	×
Respiratory diseases	×	×
External causes	×	×
Diabetes		×
Digestives diseases	×	
Mental diseases	×	
Neonatal deaths		×

Table 2: Causes of death in each dataset

The compilation method of Dataset 1 is described in Lu et al. (2014). See also Labit Hardy (2016) for a detailed description of the dataset. Those data have also been used in papers focusing on the study of mortality improvements and healthy life expectancy by deprivation level (e.g. Bajekal (2005), Lu et al. (2014)) or in mortality modeling (e.g. Villegas and Haberman (2014) and Li et al. (2017)).
In addition to updating the data for years 2007-2015, Dataset 2 provides disaggregated data by single year of age as well as data for ages below 25. This constitutes an important contribution to our paper, by allowing for a more precise analysis of the population by deprivation level.

2.2 Data analysis

The following analysis of the data shows an important heterogeneity in the composition of different age classes for both males and females, combined with significant temporal changes in composition by age, such as the striking evolution of the composition of older age classes (in particular for the age group 65-74). In particular, one might also wonder

[4]In Dataset 2, cardiovascular diseases are divided in ischemic heart diseases, strokes and other cardiovascular diseases; external causes in intentional and unintentional injuries.

how the increase in deprivation observed among younger cohorts will impact future mortality in England. While significant changes of composition occurred in the population, the gaps in mortality by deprivation level have widened. Thus, heterogeneity impacts mortality rates differently according to age or time, and generates additional complexity in the study of aggregated death rates. When results are similar, only data for males are presented for conciseness.

2.2.1 Population composition

Age Pyramids In order to illustrate differences in the composition of populations per deprivation quintile at all ages, age pyramids of the least deprived quintile (IMD Q1) and most deprived quintile (IMD Q5) are represented in Figure 1 for years 2001[5] and 2015, along with the age pyramid of England. By reading Figure 1 vertically, we can see that for each year, the form of the age pyramids vary significantly between the deprivation quintiles and the English population. IMD Q5 represented in Figure 1e and 1f, is much younger on average than IMD Q1, which is represented in Figure 1c and 1d. For instance, the median age in 2015 was 33 years (mean 35.5) in IMD Q5, while the median in IMD Q1 was 44.2 (42.6) and 39 years (39.7) in England. One factor explaining these differences could be the natural life-course trajectory of individuals, with young adults (around 20-35) typically living in rented housing in inner-city areas and with older households (older than 35) moving out to less deprived neighbourhoods.
Some cohorts are also more represented among a particular subpopulation. For instance, the English baby-boom generation (born in the years after World War II) are strikingly more represented among IMD Q1.
The horizontal reading of Figure 1 shows that in addition to this heterogeneity in age, significant temporal changes in the age pyramids occurred from 2001 to 2015. These changes are caused by population ageing, but likely also by changes in birth patterns, coupled with internal and external migrations[6]. Furthermore, changes over time in population age-structure are quite different according to the level of deprivation. For instance, the median age in IMD Q5 has dropped over 1%, from 33.4 to 33 years, while it has increased more than 9% in IMD Q1, from 40 to 44, and about 5% in the general population, from 37.1 to 39. Thus, IMD Q5 has become more youthful from 2001 the 2015, despite a general population ageing.

[5]Data by deprivation level are not available before year 2001 for ages younger than 25 years old.

[6]Here, we refer to internal migrations as the migration of individuals in between IMD quintiles (linked here to residential mobility), whereas external migrations correspond to the migration of individuals from/to places outside of England.

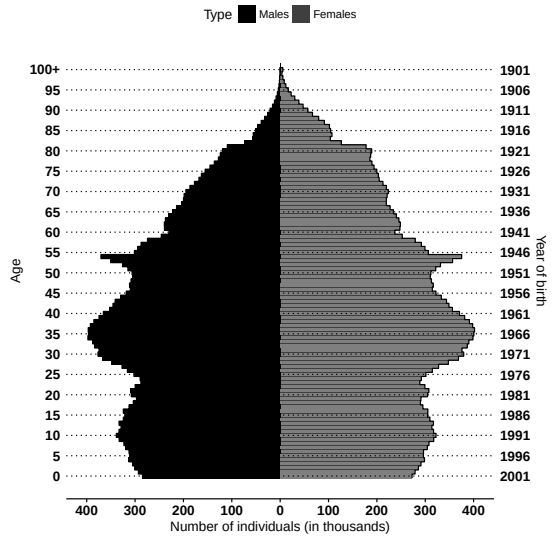

(a) English population, 2001

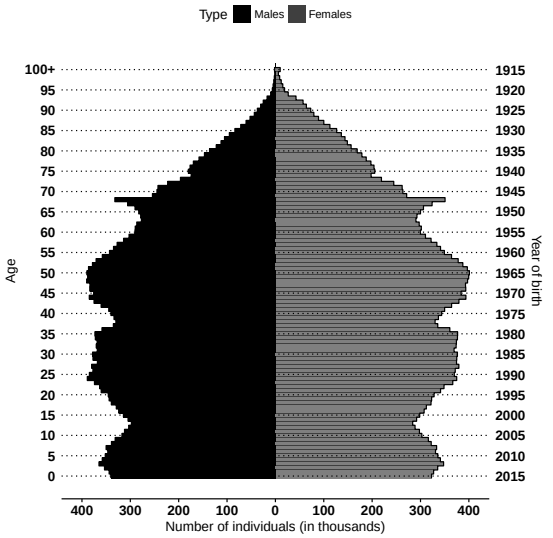

(b) English population, 2015

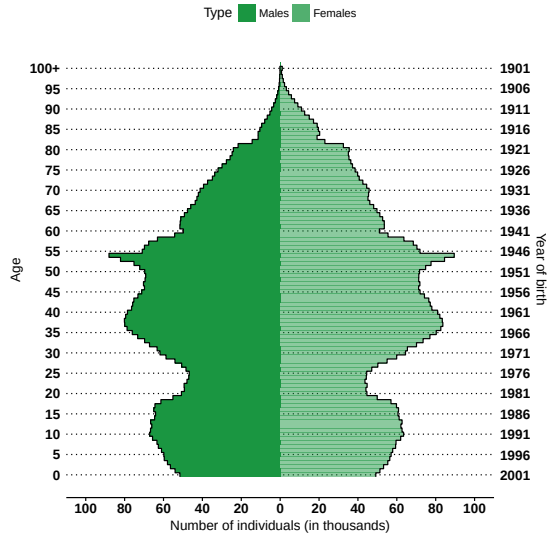

(c) Least deprived quintile (IMD Q1), 2001

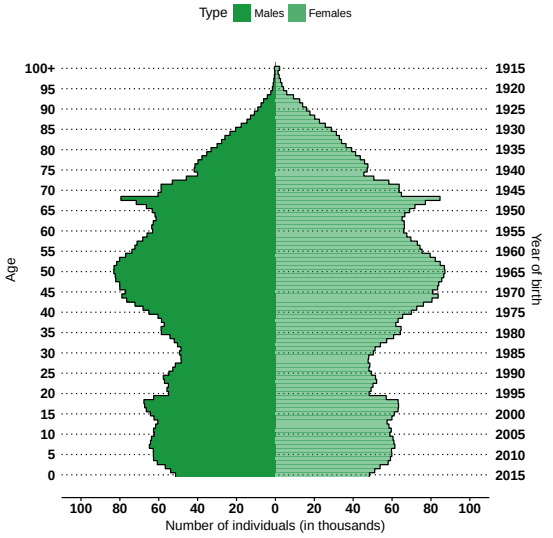

(d) Least deprived quintile (IMD Q1), 2015

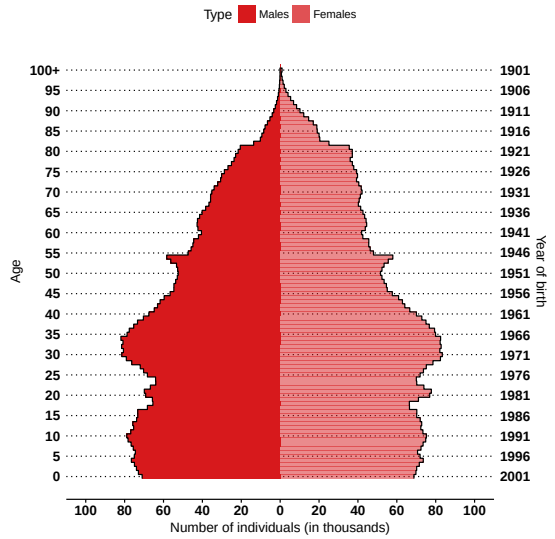

(e) Most deprived quintile (IMD Q5), 2001

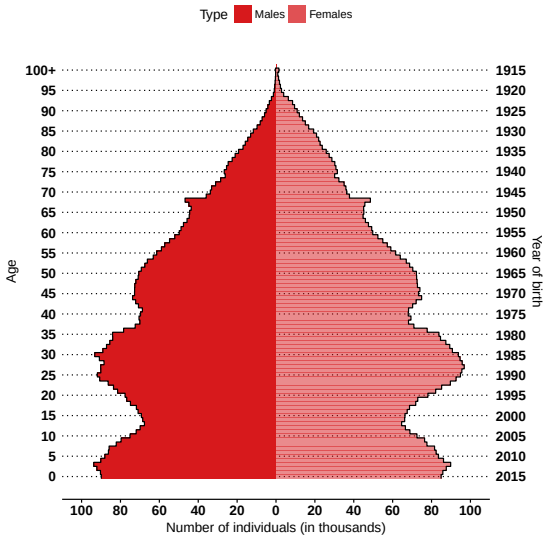

(f) Most deprived quintile (IMD Q5), 2015

Figure 1: Age pyramids in 2001 and 2015

Fixed age classes As shown in Figure 2a, the composition of age class 65-74 varied significantly from 1981 to 2015, to the benefit of the least deprived populations. In particular, the total proportion of males in the two least deprived quintiles (IMD Q1 and Q2) increased from 38% in 1981 to 46% in 2015. On the contrary, the total proportion of males in the two most deprived quintiles (IMD Q4 and Q5) decreased from 41% to 32%. This could be explained by an improvement over time of living conditions for older individuals (which could be partly due to improvements in home ownership, financial security or employment for the elderly), and also, as noted above, by a baby-boom cohort effect[7]. Indeed, over the observed period and regardless of global improving trends, individuals born during the English baby-boom are less deprived than the immediately preceding and following cohorts.

Figure 2b shows that the average level of deprivation is higher in the age class 25-34 than in the age class 65-74, this being true for the whole period 1981-2015. Moreover, the composition of age class 25-34 also varied from 1981 to 2015 (Figure 2b), with the relative deprivation of this age class increasing over time. For instance, the proportion of males in age class 25-34 for IMD Q1 and Q2 has decreased from 36% to 31%, while the proportion of males in IMD Q4 and Q5 has increased from 43% to 49%.

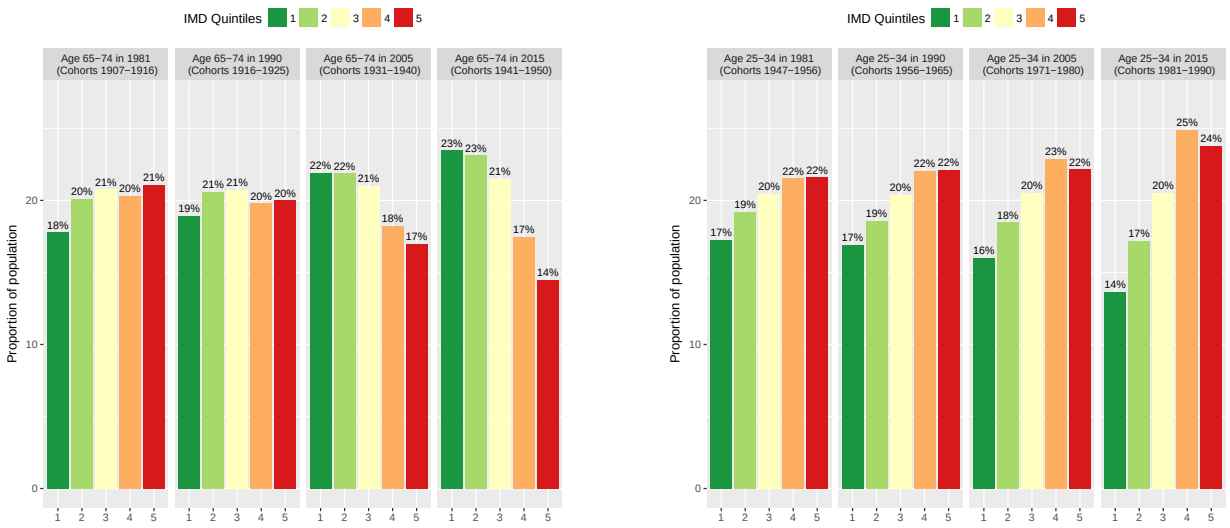

(a) Age class 65-74 (b) Age class 25-34

Figure 2: Proportion of males by age class and IMD quintile (1981, 1990, 2005, 2015)

Fixed cohorts As shown in Figure 3[8], the average level of deprivation of the 1956-60 and 1976-80 cohorts decreased over time, due to internal and external migrations[9] and differing mortality rates. However, the improvement in deprivation level for the older cohort (Figure 3a) is much higher than that of the younger cohort (Figure 3b), which confirms remarks made above regarding of Figure 2b. The proportion of males in the

[7]For more details, see e.g. Kontopantelis et al. (2018), Office for National Statistics (2018a) and Office for National Statistics (2018b).

[8]The 1976-80 cohort could only be represented up to ages 35-39.

[9]Internal migrations correspond to residential mobility.

1956-60 cohort at age 35-39, for the two most deprived quintiles, was 39%, against 43% for the 1976-80 cohort at the same age (in 2015). Similarly, the proportion in the two least deprived quintiles was about 41% in the oldest cohort (1956-60) against 37% in the youngest cohort (1976-80).
Due to differences in mortality rates, less deprived individuals naturally survive longer, and therefore at older ages the cohorts become progressively less deprived (Figure 17 in Appendix B.1).

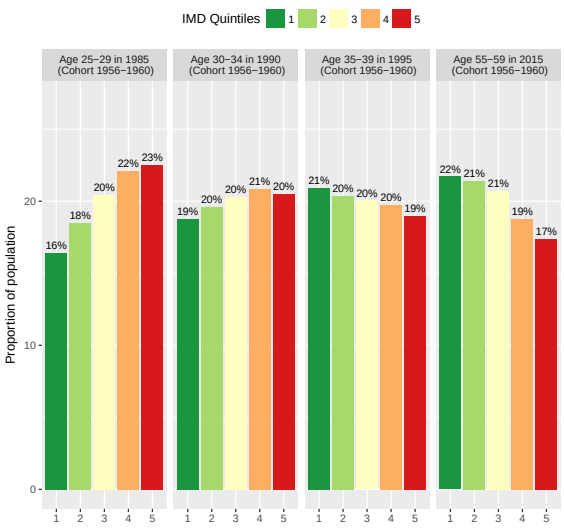

(a) Cohort 1956-60 (1985, 1990, 1995, 2015)

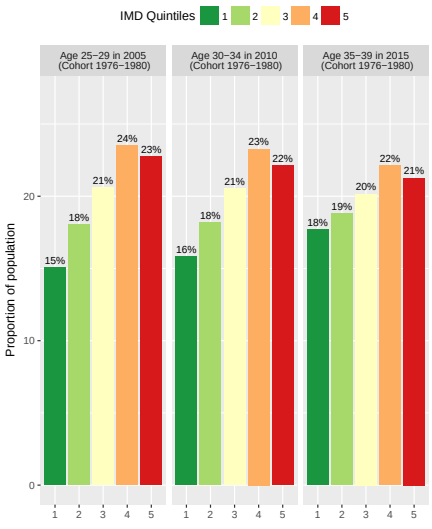

(b) Cohort 1976-80 (2005, 2010, 2015)

Figure 3: Proportion of males by cohort and IMD quintile

2.2.2 Mortality

As mortality data are more commonly studied, we only give here a brief overview of the main stylized facts, with a particular focus on Dataset 2. For more details on the mortality data, we refer to Bajekal (2005), Lu et al. (2014) or Villegas (2015) for Dataset 1 and Li et al. (2017) for Dataset 2.

Both levels and shapes of central death rates vary with the deprivation level, with mortality higher at all ages for IMD Q5 (Figure 18, Appendix B.2). Before age 35-40 (with the exception of age 0), differences are less pronounced and central death rates in all IMD quintiles are lower than 1‰. When infant mortality is not taken into account, central death rates first attain the level of 10‰ at age 58 for males in IMD Q5 (62 for females), while this value is only attained at age 68 for males in IMD Q1 (72 for females).
Despite a common improvement for all IMD quintiles, the gap in life expectancy between IMD quintiles appears to have widened over time (Figure 4). For instance, the gap in life expectancy between IMD Q1 and Q5 has grown from 2.2 years for females and 2.9 years for males in 1981, to 4.2 and 3.9 years in 2015, respectively.

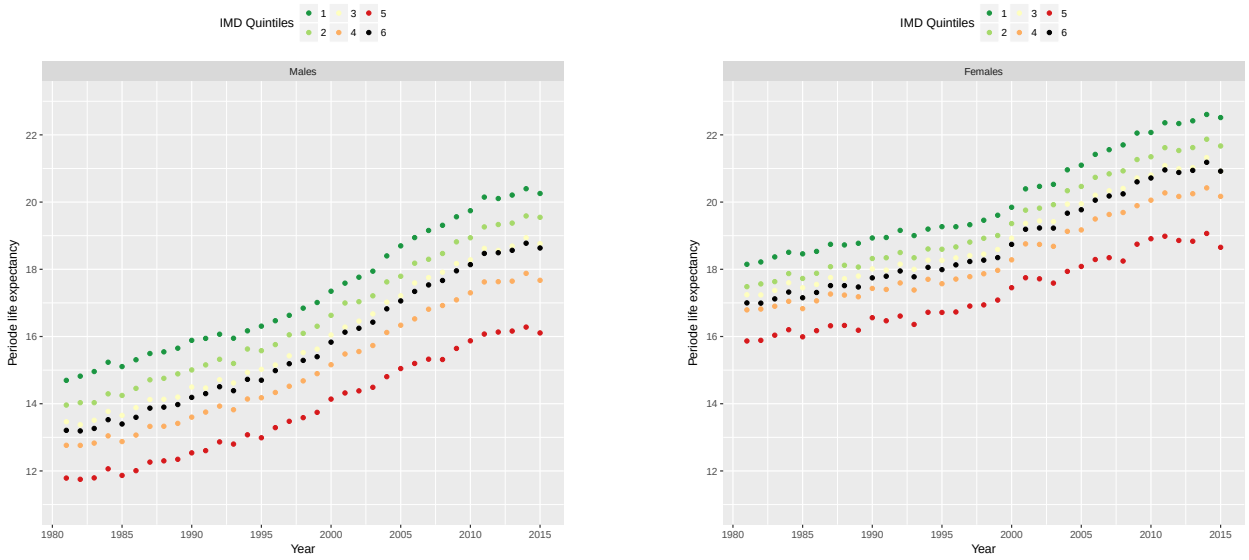

(a) Males (b) Females

Figure 4: Period life expectancy at age 65 over 1981-2015

Improvement rates Figure 5[10] shows that at all ages above 25, IMD Q5 has experienced lower rates of improvement in mortality than IMD Q1 (with the exception of age group 25-34 for females). Males experienced overall higher improvement in mortality than females, with the highest differentials in deprivation being at ages 40-44 and 45-50. Females experienced the highest differentials in the rate of mortality improvement at ages 35-39 and 40-44. Figures 6a and 6b illustrate a clear widening of the gap in annual mortality improvement at older ages, which is consistent with the observations of Lu et al. (2014) and Villegas and Haberman (2014) over the period 1981-2007 and Li et al. (2017) over the period 2001-2015 for ages above 60.

Over the period 1981-1995, males in the two most deprived quintiles (IMD Q4 and Q5) actually experienced a deterioration of mortality at ages under 40 (negative average annual rate of improvement in mortality), while improvements in mortality over the period 2001-2015 are positive (and higher for IMD Q5 under age 30). At ages above 60, the gap in mortality improvement rates increased significantly, with the highest differentials being at ages 75-79 and 80-84 for the period 2001-2015 (30-34 and 35-39 over the period 1981-1995). Improvement rates in mortality at younger ages have also changed significantly.

It is worth noting that over the period 2001-2015 and for females aged above 65, the gap in mortality improvement rates between IMD Q1 and Q5 was higher than for males (see Appendix B.3 Figure 19). This can be explained by a sharp deceleration of mortality improvement for females in IMD Q5, already reported by Villegas and Haberman (2014) for the period 1981-2007. A discussion on the potential drivers of these widening socioeconomic gaps can be found in El Karoui et al. (2018) or Lu et al. (2014).

[10]Improvement rates are computed as the yearly improvement rates of central death rates over 5-year age classes. In these graphs, improvement rates are smoothed for visualization purpose only.

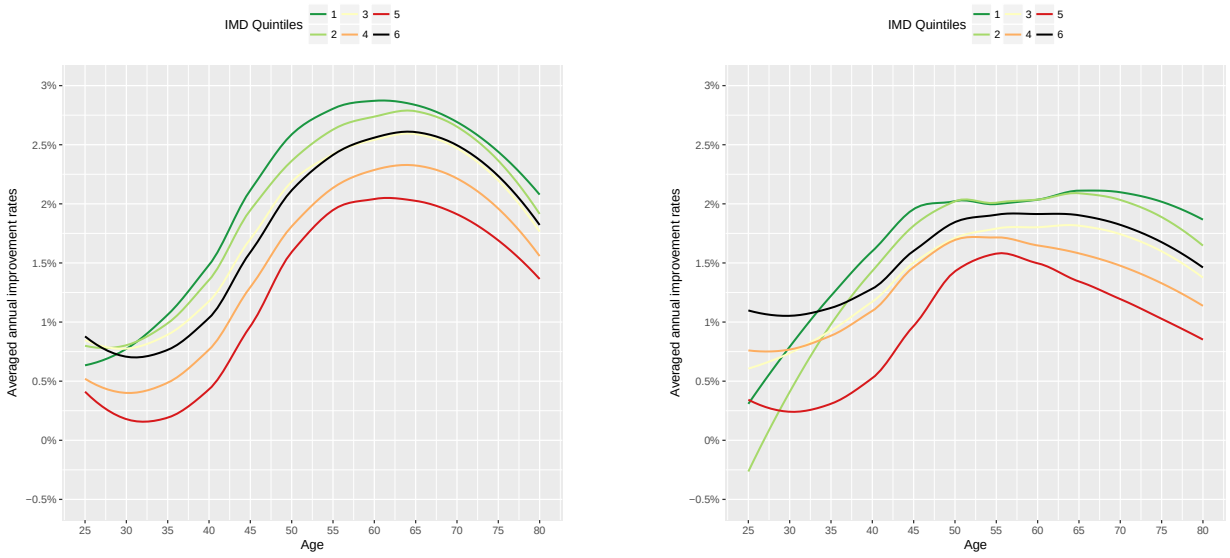

(a) Males (b) Females

Figure 5: Average annual rates of improvement in mortality, 1981-2015

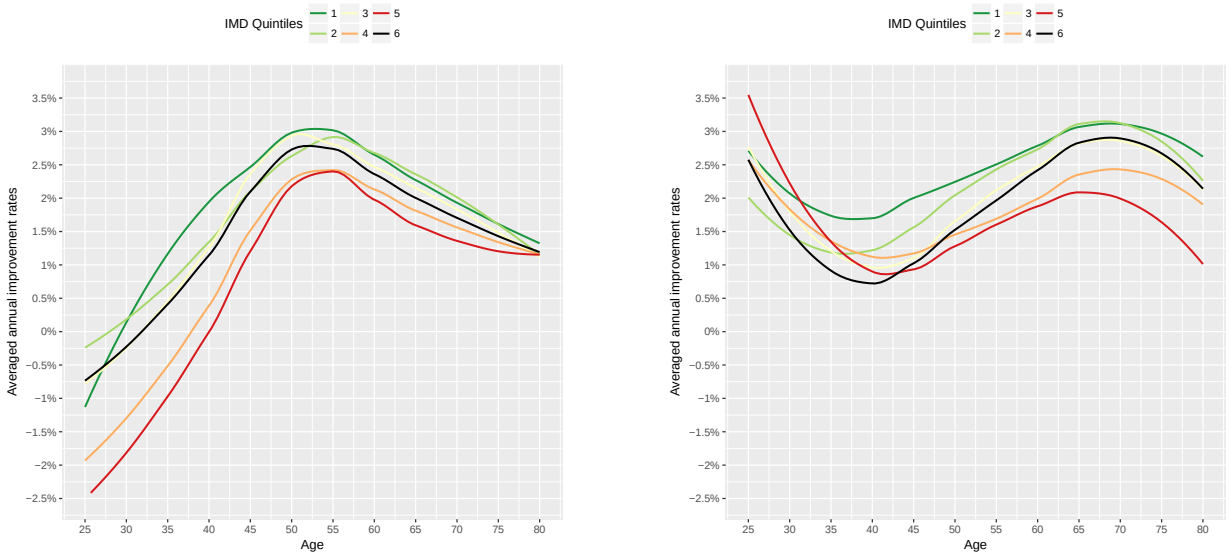

(a) 1981-1995 (b) 2001-2015

Figure 6: Average annual rates of improvement in mortality, males

Causes of death In average, cardiovascular diseases (CVD) constituted the leading cause of death for ages above 25 over the period 1981-2015, followed by cancers (neoplasms) and respiratory diseases. However, recent changes in cause of death trends have been observed since the early 2000s, with neoplasms becoming the leading cause of death, ahead of CVD. The speed of this evolution has differed by deprivation degree, gender and age class. For example, for males of age 25-85 in IMD Q1, neoplasms became the leading cause of death in 2005, while it only became the leading cause of death in 2010 for males in the same age class in IMD Q5.

Differences in cause-of-death mortality by deprivation level can mainly be observed for

neoplasms, CVD and respiratory diseases. For example, in 1981, differences between IMD Q1 and Q5 were mainly in CVD for ages 25-85 (52% of all deaths for IMD Q1 and 48% for Q5, see Figure 7), while differences were mostly in neoplasms in 2015 (40% of all deaths for IMD Q1 and 32% for Q5). For respiratory diseases, differences in the proportion of deaths remained rather stable during the whole period. Plots for females are available in Appendix B.4.

It is interesting to note as well that at young ages, the most deprived quintiles are more affected by neonatal deaths and accidents (see e.g. Oakley et al. (2009); Guildea et al. (2001) for more details on mortality at younger ages). We also refer to Villegas (2015) for more details on trends in cause-of-death mortality by deprivation level over the period 1981-2007.

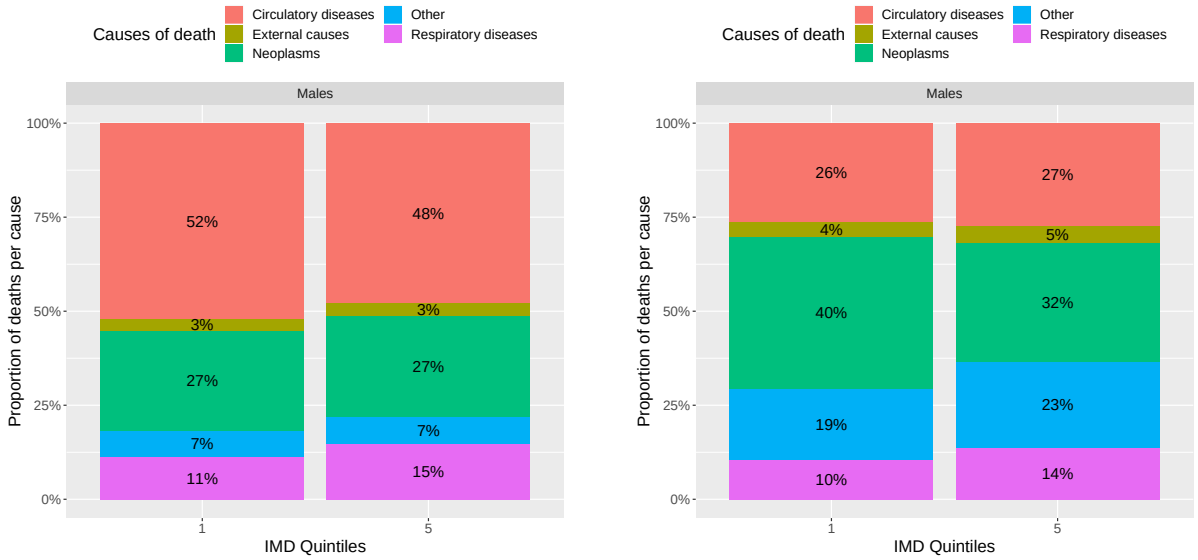

(a) 1981 (b) 2015

Figure 7: Male deaths by cause and IMD quintile for ages 25-85

3 Population dynamics model

Based on the data analysis, modeling the population dynamics appears to be instrumental to better understand the impact of heterogeneity and its evolution on the aggregate mortality. Age-structured population dynamics models take into account the information contained in the population age-structure and model its evolution.

In this study, joint evolution of the subpopulations (IMD quintiles in our case) is modeled by a linear and deterministic McKendrick-Von Foerster (McKendrick (1926); Von Foerster (1959)) with time-dependent fertility and mortality rates. We first recall briefly the McKendrick-Von Foerster model for a two-sex population, then then describe the joint evolution of the subpopulations and of the population on aggregate, and finally discuss model validation and limitations.

3.1 McKendrick-Von Foerster population dynamics model

The McKendrik-Von Foerster model is a classical age-structured deterministic population model, which can be easily adapted into a two-sex model with time dependent parameters. The model is continuous in age and time, and the population is described at time t by the function of gender and age $(g(\epsilon, a, t))$, for $a \in [0, a^\dagger[$ and $\epsilon = f$ or m respectively for females and males. $g(\epsilon, a, t)$ should be understood as the number of individuals of gender ϵ between age a and $a + \mathrm{d}a$ at time t. It follows that $\int_0^{a^\dagger} g(\epsilon, a, t)\mathrm{d}a$ is the total number of individuals of gender ϵ in the population at time t. Demographic rates are considered as parameters of the model. Coupled to an initial age pyramid, they are the determinants of the future shape of the age pyramid.

3.1.1 Demographic rates

(i) *Mortality rates:* For each gender ϵ, the mortality rate (or force of mortality) at age a and time t is denoted by $\mu(\epsilon, a, t)$. Two types of mortality indicators are usually computed, cohort indicators and period indicators:

- The period survival function is denoted $S(\epsilon, a, t) = e^{-\int_0^a \mu(\epsilon,x,t)\mathrm{d}x}$ and represents the probability to survive to age a, in the mortality conditions of time t. The period life expectancy at age a and time t is given by:

$$e(\epsilon, a, t) = \int_a^{a^\dagger} e^{-\int_a^x \mu(\epsilon,s,t)\mathrm{d}s}\mathrm{d}x = \frac{1}{S(\epsilon, a, t)} \int_a^{a^\dagger} S(\epsilon, x, t)\mathrm{d}x.$$

- The cohort survival function is denoted by $\mathcal{S}^c(\epsilon, a, t) = e^{-\int_0^a \mu_j(\epsilon,s,t-a+s)\mathrm{d}s}$, and represents the probability for an individual born at time $t - a$ to survive until age a. The cohort life expectancy, which is the average time that individuals born at time $t - a$ will live after age a, conditional to surviving to this age, is denoted by:

$$\mathcal{E}^c(\epsilon, a, t) = \int_a^{a^\dagger} e^{-\int_a^x \mu(\epsilon,s,t-a+s)\mathrm{d}s}\mathrm{d}x = \frac{1}{\mathcal{S}^c(\epsilon, a, t)} \int_a^{a^\dagger} \mathcal{S}^c(\epsilon, x, t)\mathrm{d}x.$$

We also denote by $S(\epsilon, a - x, a, t)$ and $\mathcal{S}^c(\epsilon, a - x, a, t)$ the respective period and cohort survival probabilities from age $a - x$ to age a at time t, with $S(\epsilon, 0, a, t) = S(\epsilon, a, t)$ (the same holds for $\mathcal{S}^c$).

The period and cohort indicators do not provide the same information. The cohort life expectancy is "real", in the sense that it gives information on particular individuals living in the population. On the contrary, the period life expectancy is only an indicator which aggregates information on all individuals living in a given population at a specific date t. It can be interpreted as "the average duration of life of a representative individual living in the mortality conditions of time t".

(ii) *Fertility rate*: The fertility rate for an individual with gender ϵ and age a at time t is denoted by $b(\epsilon, a, t)$. In a two-sex population, modelling births can be quite complex (Iannelli et al. (2005), Boumezoued et al. (2018)). In this article, we adopt the usual assumption that only women give births, so that $b(m, a, t) = 0$. Females are assumed to give birth to a female with a probability $p^f = p$ and to a male with probability $p^m = 1 - p$. For sake of simplicty, the female birth rate $b(f, a, t)$ is now denoted by $b(a, t)$.

3.1.2 McKendrick-Von Foerster transport equation

The evolution of the population is given by the solution of the following transport partial differential equation:

$$(\partial_t + \partial_a) g(\epsilon, a, t) = -\mu(\epsilon, a, t) g(\epsilon, a, t), \ \forall a, t > 0 \qquad \text{(balance law)} \quad (1)$$

$$g(\epsilon, 0, t) = p^\epsilon \int_0^{a^\dagger} b(a, t) g(f, a, t) \mathrm{d}a \qquad \text{(birth law)} \quad (2)$$

$$g(\epsilon, a, 0) = g_0(\epsilon, a) \qquad \text{(initial population)}$$

Intuitively, a proportion $\mu(\epsilon, a, t)\mathrm{d}t$ of individuals of age a and gender ϵ dies time t and $t + \mathrm{d}t$, and women of age in $[a, a + \mathrm{d}a[$ give birth to $b(a, t)g(f, a, t)\mathrm{d}a$ individuals at t. Equations (1)-(2) are usually solved along its characteristic curves, or cohorts lines. The resolution method can be interpreted as counting the number of survivors at time t in each cohort. Two regimes can be distinguished:

(i) *Individuals present in the initial population* ($a \geqslant t$): At time t, individuals who were already present in the initial population are individuals of age $a \geqslant t$. Their number at time t is the number of individuals of age $a - t$ in the initial population who survived until time t:

$$g(\epsilon, a, t) = g_0(\epsilon, a - t)\mathcal{S}^c(\epsilon, a - t, a, t), \quad a \geqslant t. \tag{3}$$

(ii) *Individuals born after the initial time* ($a < t$): At time t, individuals born after $t = 0$ are individuals of age $a < t$. Their number at time t is thus the number of individuals born at time $t - a$ and who survived until time t:

$$g(\epsilon, a, t) = p^\epsilon B(t - a)\mathcal{S}^c(\epsilon, a, t), \quad a < t, \tag{4}$$

where $B(t)$ is the number of individuals born at time t:

$$B(t) = \int_0^{a^\dagger} b(a, t) g(f, a, t) \mathrm{d}a. \tag{5}$$

Thus, if we look at the population at a small time t, the age pyramid will be mostly shaped by the time translated initial age pyramid, and will follow the idea that "today's youths give us most of the information on tomorrow's seniors". On a longer term, the initial population is naturally erased and the shape of the future age pyramid is only characterized by the birth function B and survival functions.

Stable solution of the McKendrick-Von Foerster equation The stable theory defines a *stable age profile*, given a fixed regime of time-independent age-specific demographic rates (see Keyfitz and Caswell (2005), Inaba (2017), or Webb (1985) for a more general framework). Similarly to the period life expectancy, the stable age profile gives information on a fictive population, living *in the mortality and fertility conditions of a given time*. For instance its comparison with the real age profile of the population allows us to observe if strong changes in birth or mortality rates have occurred in the past.

A stable solution (for females) of the McKendrick-Von Foerster evolution Equation (1)-(2)

with time independent demographic rates $\mu(\epsilon, a)$ and $b(\epsilon, a)$, is a solution which can be expressed as a product function $e^{-\lambda^* a - \int_0^a \mu(f,x)\mathrm{d}x} C_0 e^{\lambda^* t}$, where λ^* is the unique solution of:

$$1 = p^f \int_0^{a^\dagger} b(a) e^{-\lambda^* a - \int_0^a \mu(f,x)\mathrm{d}x} \mathrm{d}a. \tag{6}$$

The previous equation is called the characteristic equation and λ is called the intrinsic growth rate of the population. A solution of this type is called stable because its age profile, or age distribution, remains constant over time, in the sense that the proportion of individuals in each age class remains constant.
An important property is that the solution of (1-2) with time independent demographic rates behaves asymptotically as a stable solution. After a long period of time, the population increases or decreases exponentially at rate λ^*, and

$$g(\epsilon, a, t) \underset{t\to\infty}{\sim} p^\epsilon C(\lambda^*, g_0) e^{\lambda^*(t-a)} S(\epsilon, a). \tag{7}$$

Equation (7) can be interpreted as follows: at a given time t_0, the right hand side of the equation is the shape that the age pyramid at t_0 would have if the demographic rates had been constant in the past, equal to $\mu(a, t_0)$ and $b(a, t_0)$.

3.2 Joint evolution of the subpopulations

3.2.1 Subpopulations evolution

In the sequel, we consider the evolution of p socioeconomic subpopulations (for instance IMD quintiles). For each $j = 1...n$, the population j is described by the solution g_j of the McKendrick-Von Foerster Equations (1)-(2) with initial population g_0^j and demographic rates $\mu_j(a, t)$ and $b_j(a, t)$, where $g_j(\epsilon, a, t)$ is the number of individuals at time t in population j, gender ϵ and between age a and $a + \mathrm{d}a$.

3.2.2 Aggregated population

We call aggregated population the global population composed of all subpopulations, denoted by $g(\epsilon, a, t)$ with:

$$g(\epsilon, a, t) = \sum_{j=1}^{n} g_j(\epsilon, a, t).$$

The aggregated population dynamics is thus defined by

$$(\partial_t + \partial_a) g(\epsilon, a, t) = -\sum_1^n \mu_j(\epsilon, a, t) g_j(\epsilon, a, t), \quad g(\epsilon, 0, t) = p^\epsilon \int_0^{a^\dagger} (\sum_1^p b_j(a, t) g_j(f, a, t)) \mathrm{d}a.$$

Aggregated mortality The mortality rate at age a in the aggregated population corresponds to the intensity of individuals aged a (for each gender) dying between a short interval of time $\mathrm{d}t$. Here, the previous partial differential equation can be rewritten as:

$$(\partial_t + \partial_a) g(\epsilon, a, t) = -\left(\sum_1^n \mu_j(\epsilon, a, t) \frac{g_j(\epsilon, a, t)}{g(\epsilon, a, t)} \right) g(\epsilon, a, t).$$

The mortality rate of the aggregated population is thus:

$$d(\epsilon,a,t)=\sum_{j=1}^{n}\mu_j(\epsilon,a,t)w_j(\epsilon,a,t),\ \text{with}\quad \omega_j(\epsilon,a,t)=\frac{g_j(\epsilon,a,t)}{g(\epsilon,a,t)}. \tag{8}$$

Actually, the mortality rate in the aggregated population should be denoted by $d(\epsilon,a,t,(g_j)_{j=1..p})$, since it depends on the age pyramids of all subpopulations. The time dependence of the aggregate mortality rate is caused not only by the time-dependence of the specific mortality rates in each subpopulation, but also by the evolution of the proportions $w_j(\epsilon,a,t)$ of individuals in each subpopulation and age class.
In order to better understand how these weights could impact the aggregated population, let us again make the distinction between the two cases $a \geqslant t$ and $a < t$. In order to simplify notations, we consider for the remainder of this section that the aggregated population is composed of two subpopulations ($p = 2$). When there is no ambiguity, we also omit the gender variable ϵ.

Aggregated mortality over the short term For individuals present in the initial population (of age $a \geqslant t$ at time t), the age pyramid of the subpopulations are mostly shaped by the initial subpopulations and Equation ((3)) yields for $a \geqslant t$:

$$d(a,t)=\frac{g_0^1(a-t)\mathcal{S}_1^c(a-t,a,t)\mu_1(a,t)+g_0^2(a-t)\mathcal{S}_2^c(a-t,a,t)\mu_2(a,t)}{g_0^1(a-t)\mathcal{S}_1^c(a-t,a,t)+g_0^2(a-t)\mathcal{S}_2^c(a-t,a,t).} \tag{9}$$

For small times t, the previous equation holds for most ages and the aggregated mortality depends on three factors:
- The subpopulations mortality rates μ_1 and μ_2.
- The initial subpopulations g_0^1 and g_0^2: the aggregated mortality rate at age a depends on the initial composition of the age class $a-t$, since individuals are assumed to stay in the same subpopulation. In particular, if the initial age pyramid is very heterogeneous in age, i.e. if the age classes are composed very differently, aggregate death rates could experience significant changes (for instance if younger individuals are more deprived than older ones, this could lead to an increase in aggregated mortality rates).
- Cohorts survival: if the initial age pyramids in each subpopulation are equal ($g_0^1 = g_0^2$) Equation ((9)) becomes:

$$d(a,t)=\frac{\mathcal{S}_1^c(a-t,a,t)\mu_1(a,t)+\mathcal{S}_1^c(a-t,a,t)\mu_2(a,t)}{\mathcal{S}_1^c(a-t,a,t)+\mathcal{S}_2^c(a-t,a,t)}\quad a\geqslant t.$$

This illustrates a well known "selection" effect which is that if a subpopulation, say subpopulation 2, experiences a higher overall mortality, Subpopulation 1 will have more and more weight at older ages and the aggregated mortality will tend to the mortality rate of Subpopulation 1.

Aggregated mortality over the long-term On a longer term, the subpopulations evolution are mainly governed by the birth functions B_1 and B_2 and for $t > a$:

$$d(a,t)=p^{\epsilon}\frac{B_1(t-a)\mathcal{S}_1^c(a,t)\mu_1(a,t)+B_2(t-a)\mathcal{S}_2^c(a,t)\mu_2(a,t)}{B_1(t-a)\mathcal{S}_1^c(a,t)+B_2(t-a)\mathcal{S}_2^c(a,t)}. \tag{10}$$

Thus, if the subpopulations experience heterogeneity in birth patterns for a certain period of time, this can induce a temporary variation in the aggregated mortality rates and generate a so-called *cohort effect*.

3.3 Model validation and limitations

Details on the numerical implementation of the model can be found in Appendix C.
Due to the lack of data availability, internal and external migrations are not taken into account in the modeling, which can be unrealistic for young adults, but appears plausible for older age classes. In order to test this hypothesis, we have simulated population evolution using the historical demographic time-dependant rates and compared the final simulated pyramid with the actual historical pyramid available from the data. Subpopulation evolution was first (Case 1) simulated from years 1981 to 2011, using 5-year age class inputs (initial pyramid and demographic rates available only after age 25)[11]. Secondly (Case 2), we simulated subpopulation evolution for all ages from years 2001 to 2015, using 1-year age class inputs[12]. We compared individuals after age 40, for which migrations are less significant. This corresponds for Case 1 to individuals aged between 70 and 85 in 2011 (40 and 55 in 1981), and to individuals aged between 54 and 85 in 2015 (40 and 71 in 2001) for Case 2. For Case 1, the average relative difference in the number of individuals by gender, deprivation quintile and age class, between the simulated and historical pyramids, is at most 4%, except for females in IMD Q5, for which it is 6.8%. For Case 2, it is at most 3%, except for females in IMD Q5, for which it is 5.2%. For both Cases 1 and 2, relative differences in the proportions of individuals within each subpopulation have similar magnitudes as the average relative differences in the number of individuals in each subpopulation. However, when considered at aggregate level, the average relative difference in the number of individuals per age class is only 1.5% for males and 0.5% for females in Case 1, and 1% for males and 0.7% for females in Case 2. The additional deviation that arises when looking at subpopulation differences could be partly attributed to the absence of a mechanism capturing small existing internal migrations at ages above 40. Even without accounting for this, the simulated and historical pyramids remain largely consistent at both aggregate and subpopulation levels, for ages initially above 40. Moreover, using 1-year age class inputs lowers the differences between the simulated and historical pyramids (Case 2). Indeed, even though the simulation period is shorter in Case 2, the age range tested is wider than when using the 5-year age class inputs in Case 1.

Thus in its current implementation, the model can predict well the population evolution of individuals older than 40 years old at initial year of simulation. However, it would require extension to accurately project for individuals younger than 40 years old. For these individuals, migrations should be considered, as well as a birth rates forecasting model for newborns. Currently, the model does not account for the full complexity of

[11] This simulation period is used for one application presented in Section 4.1

[12] Due to the databases characteristics, the largest possible period to simulate with a 1-year age class inputs for all ages is 2001-2015, see the databases characteristics in Table 1.

the population evolution; however, it is worth repeating that the framework used in this study is not intended to be a predictive tool, but rather a tool for experimenting and simulating different scenarios. Indeed, even in this streamlined framework, we are able to reproduce composition changes and capture non-trivial effects of the heterogeneous population dynamics, presented in Section 4. Moreover, this framework allows the derivation of quasi-explicit formula and asymptotic results for a number of indicators, allowing for easier interpretation.

4 Numerical Results

In order to illustrate different potential impacts of heterogeneity on the mortality experienced by the aggregated population, we now apply the model presented in Section 3.
We first show in Section 4.1 how within-age heterogeneity (of, in our case, deprivation levels) can impact the aggregate population mortality. Then, in Section 4.2, we show how the effects of a cause of death reduction could be compensated for by population composition changes induced by a cohort effect, and thus how it could be misinterpreted when the population heterogeneity is not taken into account.
For illustrative purposes, we consider in the remainder of this section the evolution of a synthetic heterogeneous population composed of two subpopulations: the most and least deprived IMD quintiles (denoted by 1 and 5 in the following). Only results for males are presented for conciseness, as results for females are similar.

4.1 Impact of heterogeneity in the initial age pyramid

As seen in Section 2.2, the English population presents a strong *heterogeneity in age*, meaning that the population composition varies substantially according to age class, and that age classe composition has also varied significantly over time. In the following, we illustrate how heterogeneity in age can impact two indicators: the period life expectancy at age 65, and mortality improvement rates above age 65.

Demographic scenario (Scenario A) In order to isolate the influence of changes in population composition, we assume for this first scenario that mortality rates in each subpopulation are time-independent. The population is simulated "on the short term" (30 and 40 years) in two cases: the initial age pyramids and mortality rates are first based on the data for year 1981, and secondly on the data for year 2015[13]. Thus, the aggregated death rate defined in Equation (8) is

$$d(\epsilon, a, t) = \sum_{j=1,5} \hat{\mu}_j(\epsilon, a, y) w_j(\epsilon, a, t), \text{ and } \quad g_0(\epsilon, a) = \sum_{j=1,5} \hat{g}_j(\epsilon, a, y), \tag{11}$$

where $\hat{\mu}_j(\epsilon, \cdot, y)$ and $\hat{g}_j(\epsilon, \cdot, y)$ are the mortality rates and age pyramid of subpopulation j fitted to the data for year $y = 1981$ or 2015.

[13]Remembering that data are structured by 5-year age classes in Dataset 1 (1981-2007), and by single year of age in Dataset 2 (2001-2015).

Remark. *Note that there is no available data for ages younger than 25 in Dataset 1 (i.e. for $y = 1981$). Hence, when $y = 1981$, individuals younger than 25 are assumed to be identically distributed in each subpopulation, based on the English age pyramid. However, this hypothesis has no influence on our results since only indicators at ages above 65 are considered, over a period of 30 or 40 years. Thus, only individuals who were initially more than 25 years old are taken into account in the computation of the aggregated indicators, and therefore fertility rates have no influence on the results either. Computations for the aggregated death rates are thus based on Equation* (9)*, which justifies our terminology "short term".*

The evolution of the aggregated populations are represented in Figure 8 (y=1981) and 9 (y=2015). Each age class is represented by the addition of individuals in the most deprived subpopulation (IMD Q5, in red) and in the least deprived subpopulation (IMD Q1, in green). The green line in each graph represents the shape of the least deprived subpopulation age pyramid. Furthermore, the two regimes in the population evolution described in Section 3.1 are distinguished by the black dashed line in the age pyramids at t=30 years (Figures 8b and 9b). Individuals aged over 30 were initially present in the population, and the corresponding age pyramids defined by Equation (3). Individuals aged under 30 were born after the initial time, and the corresponding age pyramid is defined by Equation (4).
As discussed in Section 2.2, older individuals are more deprived in the 1981 synthetic initial age pyramid than in the 2015 age pyramid. For the population based on the 1981 inputs (Figure 8), a *decrease in deprivation* can be observed for individuals over age 60, due to the fact that younger cohorts were initially less deprived than older ones. Indeed, despite important differences in mortality rates, there were initially more individuals older than 60 in the most deprived subpopulation.
On the contrary, an *increase in deprivation* can be observed in age group 45-70 for the population based on 2015 inputs (Figure 9). Initially in this age group, there were more individuals in Subpopulation 1, while the situation is reversed after 30 years, with more individuals in Subpopulation 5. The aging of the larger cohort composed of individuals initially in the age group 45-55 also induces a significant increase in the number of individuals in the age group 75-85. However, the proportion of individuals in each subpopulation appears to be rather stable over time, with around 60% of individuals in Subpopulation 1 for this age group.

Impact on the aggregated mortality In order to better understand the impact of compositional changes on the aggregated mortality, Scenario A is compared to two other scenarios (noted B and C): in Scenario B, population evolution is combined with mortality improvements in each subpopulation; in Scenario C, only mortality improvements are considered, without taking into account compositional changes (that is, the population composition is fixed, equal to the initial population composition). In Scenarios B and C, mortality improvements are modeled using a constant annual mortality improvement rate of 0.5% for all ages. This allows us to compare the order of magnitude of mortality changes induced by compositional changes, to those induced by moderate mortality improvement

rates, as well as their interplay for both $y = 1981$ and 2015.
Since mortality rates are assumed to be time-independent in Scenario A, the aggregated mortality only evolves due to changes in the subpopulation age pyramids. On the other hand, the population composition is fixed in Scenario C, and thus the aggregated mortality evolves only due to the constant annual mortality improvement rate of 0.5%. In Scenario B, the aggregated mortality depends on both mortality improvement rates and population dynamics.

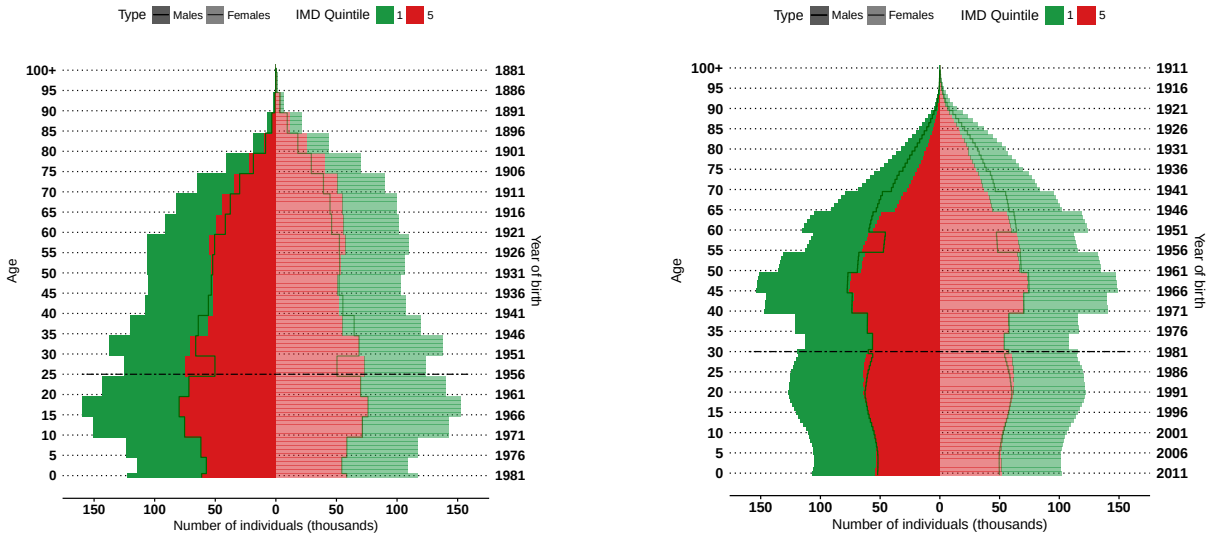

(a) Initial age pyramid (b) Age pyramid at t=30

Figure 8: Evolution of the aggregated age pyramid, $y = 1981$

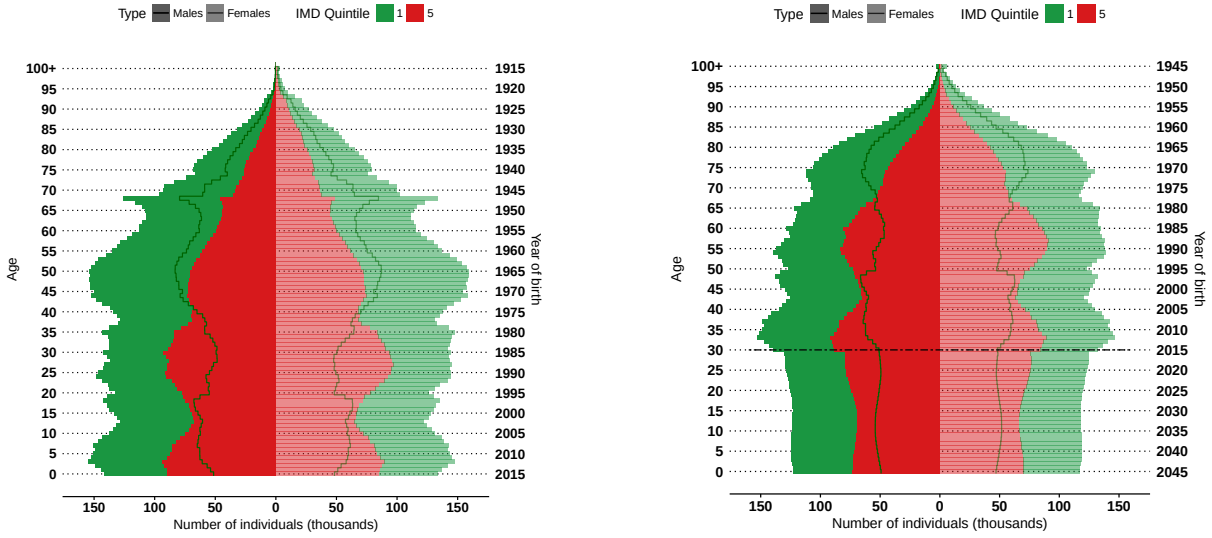

(a) Initial age pyramid (b) Age pyramid at t=30

Figure 9: Evolution of the aggregated age pyramid, $y = 2015$

Results are presented in Figure 10[14] and 11. Note that the evolution of life expectancy

[14]The axis on top of each graph represents the initial-time age of 65 years old individuals at time t.

between $t = 30$ and $t = 40$ should be interpreted with caution. Indeed, we observe significant population flows in the data for ages 25-35, resulting from both internal and external migrations. For instance, the decrease in the period life expectancy between $t = 30$ and $t = 40$ in Figure 10a is also caused by the fact that the model does not take these changes into account.

According to the initial year y of inputs, the indicators evolve in *opposite directions*.

In the conditions of 1981, period life expectancy at 65 increases for Scenario A, and average mortality improvement rates are *positive* at all ages. This means that the evolution of the population composition contributes *positively* to the aggregated mortality. This is confirmed by the period life expectancy and average mortality improvement rates in Scenario B, which are higher than in Scenario C, for which the population dynamics are not taken into account. In particular, in Scenario B, average annual mortality improvement rates are larger than 0.7% for all ages younger than 80, in comparison to the constant improvement rates of 0.5% in Scenario C. Thus, favorable changes in population composition since 1981 likely contributed to the increase in the aggregated life expectancy.

On the other hand, in the conditions of 2015, the life expectancy at age 65 in Scenario A *decreases* by approximately 6 months, after a slight increase during the first half of the simulation, with *negative* average mortality improvement rates at all ages below 80. Thus, the evolution of the least and most deprived subpopulations contribute *negatively* to the evolution of the aggregated mortality. In Scenario B, mortality improvement rates for each subpopulation are compensated for by adverse evolution of the population composition. In particular, average annual mortality improvement rates in Scenario B are lower than in Scenario C for all ages under 81. This suggests that changes in population composition might offset future improvements in subpopulation mortality rates.

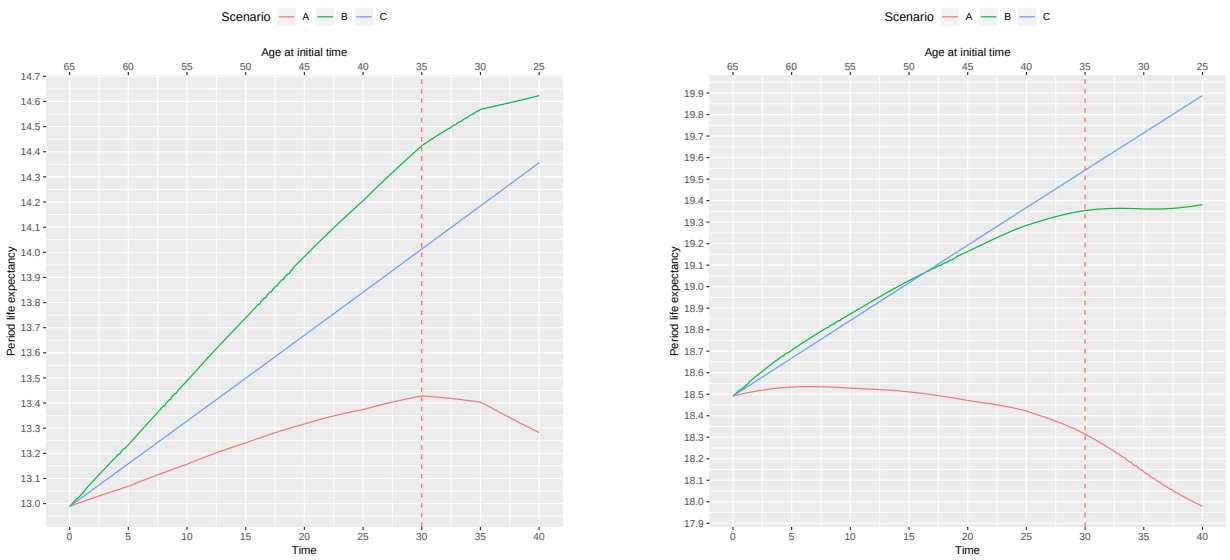

(a) 1981 inputs (b) 2015 inputs

Figure 10: Evolution of male life expectancy at age 65

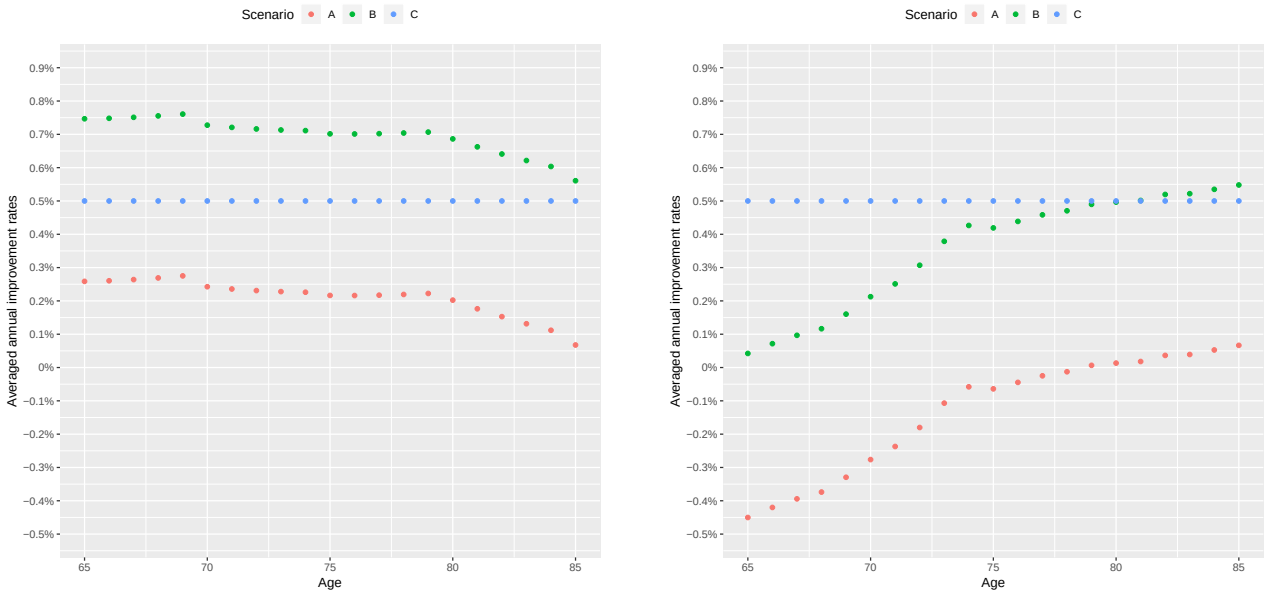

(a) 1981 inputs

(b) 2015 inputs

Figure 11: Average male annual mortality improvement rates over the simulation period 0-30 years

4.2 Cause of death reduction and compensation effect

The numerical results of the previous subsection show how changes in composition of the heterogeneous population can impact the aggregated mortality, even when mortality rates in each subpopulation do not change over time. We are now interested in studying the evolution of aggregated mortality indicators when changes of composition are coupled with a cause-of-death mortality reduction.

In the following, changes in the population composition are quantified by birth patterns, and coupled with cause-specific reduction of mortality. The classical assumption of independence between causes of death is assumed[15]. By first studying the evolution of the population dynamics when demographic rates are changed separately, we show that period and cohort indicators computed on the aggregated population are able to capture changes in mortality of different natures. Finally, the results presented at the end of the section show how a cause of death reduction could be compensated and thus misinterpreted in presence of heterogeneity, due to structural changes in the population composition.

Baseline scenario (0) We first define a baseline scenario serving as reference scenario, and for which the computed indicators are nearly constant. To that end, demographic rates are taken as time-independent in Scenario (0). The mortality rates in each subpopulation are the fitted mortality rates of year 2015: $\mu_j(\epsilon, a) = \hat{\mu}_j(\epsilon, a, 2015)$. Under this scenario, the period and cohort life expectancies in each subpopulation are thus fixed and equal to the 2015 period life expectancies. For example, the male life expectancy at age 25

[15]This assumption is discussed at the end of the section (see also Chiang (1968) or Boumezoued et al. (2018)).

is 58.1 in the least deprived subpopulation and 50.8 in the most deprived subpopulation. Fertility rates are assumed to be the same in each population and estimated from English fertility rates in 2015[16].

As we have seen in the previous results, the heterogeneity of the age pyramid can lead to significant changes in the aggregated mortality even when mortality rates are time-independent. In order to limit the influence of the initial age pyramids, a natural choice could be to consider an initial pyramid in which each all classes are composed of the same number of individuals from each subpopulation. However, this choice leads to important variations in the aggregated mortality, due to the modification of cohorts composition over time induced by differences in mortality rates between the two subopulations. Since individuals in Subpopulation 5 have higher mortality, the composition of cohorts is modified as individuals grow older, generating a change of composition in older age classes from the initial "50/50" distribution to a distribution composed of more individuals in Subpopulation 1. The solution to this issue is to choose initial pyramids which "corresponds" to the specific mortality rates of each subpopulation, that is the stable pyramids corresponding to the specific demographic rates of each supopulation, as defined in Section 3.1.2. Since fertility rates of each subpopulation are the same in the baseline scenario, the intrinsic growth rates of each subpopulation are very close. This guarantees that the composition of the aggregated population stays almost constant over time, with cohorts composed at birth of approximately 52% of individuals in the most deprived subpopulation. In particular, the aggregated male period and cohort life expectancies at age 25 under the baseline scenario are 54.3 (Figure 12).

Scenario 1a: cause of death mortality reduction In the first scenario, we consider a progressive reduction of mortality rates from Cardiovascular Diseases (CVD) (cause 2), which could be the result for instance of a targeted public policy or improvements in medical care. The initial mortality rates (at $t = 0$) in each subpopulation $j = 1, 5$ are equal to the fitted 2015 mortality rates, as in the baseline scenario, and can be written as the sum of the fitted mortality rates $\hat{\mu}^{\epsilon}_{ij}$ for the m causes of death available in the datasets:

$$\mu^{\epsilon}_{j}(a, 0) = \sum_{i=1}^{m} \hat{\mu}^{\epsilon}_{ij}(a, 2015).$$

Under Scenario 1a, mortality rates from CVD are reduced linearly over a period of $h_r = 30$ years starting from the year $t_r = 40$, in order to attain a reduction of $\alpha\%$ of CVD mortality rates at the end of the period[17]. More formally, the mortality rate at age a and year t in subpopulation j is defined as follow:

$$\mu^{\epsilon}_{j}(a, t) = \sum_{i \neq 2} \mu^{\epsilon}_{ij}(a, 0) + (1 - \alpha(t))\mu^{\epsilon}_{2j}(a, 0), \quad \alpha(t) = \mathbb{1}_{[t_r, t_r + h_r[}(t) \frac{\alpha}{h_r}(t - t_r). \tag{12}$$

The evolution of the aggregated period and cohort male life expectancies at age 25 is represented in Figure 12 under Scenario 1a, for $\alpha = 10\%, 20\%$ and 30%.

[16] English female fertility rates are estimated from Office for National Statistics (2015a), for 5-year age classes and for ages 15 to 44 (see Boumezoued et al. (2018) for more details on the estimation).

[17] The choice of values for t_r and h_r are discussed at the end of the section.

When $\alpha = 30\%$, the reduction of CVD mortality rates generates an increase of respectively 0.7 and 0.9 years for the male period life expectancy in the least and more deprived subpopulations. As a rough order of magnitude, this represents approximately 10% and 16% of the historic increase in male life expectancy over the period 1985-2015.
Due to the reduction in mortality from CVD, the aggregated male period life expectancy at 25 (Figure 12a) also experiences an increase ranging from 0.3 to 0.8 years, with a middle value of 0.6 years when the cause is reduced by 20%. It is interesting to note that the period life expectancy is more adapted than the cohort life expectancy to capture this type of mortality changes. Indeed, the period life expectancy is a period index based on the mortality of individuals living at time t, and is therefore able to capture the starting time and the period of the mortality reduction, and to some extent the magnitude of the mortality reduction. On the other hand, the cohort life expectancy, by including future mortality rates in its computation at a given time, has a smoother evolution, which makes the interpretation of underlying mechanisms more difficult.
These remarks are coherent with the classical approach to mortality modeling and forecasting, in which mortality rates are often represented by an age dependent function, whose evolution over time is described using time-series (see e.g. the short model review in Ludkovski et al. (2016)). However, if the period dimension appears to be well-suited to capture mortality changes such as a cause-of-death mortality reduction, we show in the following that variations in mortality caused by changes in population composition are not necessarily well-captured by period indexes.

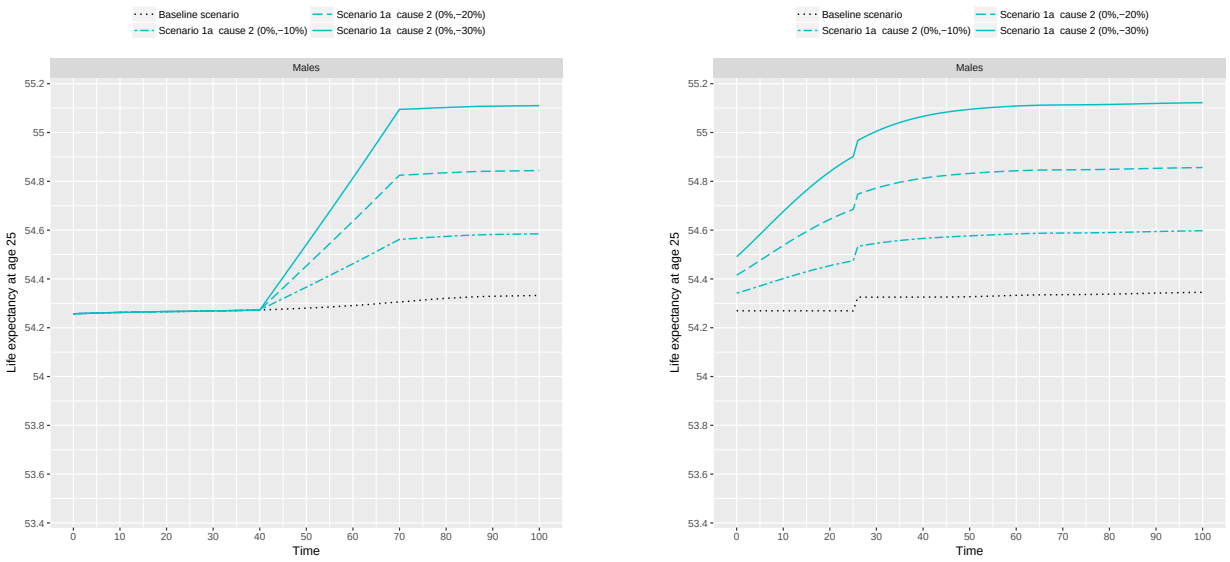

(a) Period life expectancy (b) Cohort life expectancy

Figure 12: Aggregated male life expectancy: cause-of-death reduction (scenario 1a)

Scenario 1b: 'reverse' cohort effect In the second scenario, changes in the aggregated mortality are caused changes to the population composition. These compositional changes are generated by a 'reverse' cohort effect (adverse compositional changes in particular cohorts) modeled by fertility rates which are different in each subpopulation. Over

a period h_b, the fertility rates of the most deprived subpopulation ($j = 5$) are increased of $\beta\%$:

$$b_5(a,t) = \hat{b}(a,2015)(1 + \beta \mathbb{1}_{[0,h_b[}(t)). \tag{13}$$

The evolution of the aggregated period and cohort male life expectancies at age 25 under this scenario is represented in Figure 13, for $h_b = 20$ years and $\beta = 20\%, 40\%$ and 60%. Due to the higher fertility rates in the most deprived subpopulation over the period $[0, h_b[$, the composition of the population changes and the weight of the most deprived subpopulation becomes more important in the aggregated population/mortality than in the baseline scenario. In our example, the cohorts born during the first 20 years of the simulation are respectively initially composed of 56%, 60% and 63% of individuals in the most deprived subpopulation.

Before time $t = 25$, the period life expectancy at age 25 is based on individuals present in the initial population, and since mortality rates are the same as in the baseline scenario, the two scenarios do not differ up until this time. From $t = 25$, the computation of the period and cohort life expectancy at age 25 includes individuals born during the reverse cohort effect. The increase in deprivation among the cohorts born over this period leads to a degradation of the aggregated mortality.

The cohort dimension is more adequate to capture mechanisms underlying aggregated mortality changes under this scenario. At time $t = 25$, the cohort life expectancy (Figure 13b) experiences a negative jump, which captures the sudden increase in deprivation of the cohort of individuals aged 25 at t (born at the beginning of the reverse cohort effect). The last cohort born during the reverse cohort effect attain age 25 at time $25 + h_b = 45$, corresponding to the sudden increase in the cohort life expectancy. After time t=45, the cohort life expectancy progressively decreases over 20 years, corresponding to the introduction of generations born from these more deprived cohorts. Changes of composition in these cohorts alone (which have the same mortality as in the baseline scenario) generates a decrease in the cohort life expectancy ranging from 0.3 to 0.8 years as β increases. Thus, changes in the life expectancy due to changes in the population composition are of the *same order of magnitude* as the changes caused by the cause-of-death mortality reduction of Scenario 1a.

On the other hand, the period life expectancy, which is smoother, progressively integrates individuals from the more deprived cohorts over time. It is thus difficult to understand the underlying factors responsible for the decrease in life expectancy, based only on the period index. As changes are due to differences in fertility rates, the population dynamics have to be observed on a longer term in order to see the impact of composition changes on the period life expectancy.

Scenario 2 In this last scenario, we study the combined effects of cause-of-death mortality reductions and 'reverse' cohort effects. We consider a progressive cause-of-death mortality reductions for different causes of death, with $\alpha = 20\%$, but now coupled with the 'reverse' cohort, with $\beta = 20\%, 40\%$ and 60%.

Figure 14a represents the evolution of the period life expectancy for a progressive reduction of mortality from CVD under this scenario. As in Scenario 1a, the CVD mortality

is progressively reduced from $t_r = 40$, and the period life expectancy increases over the reduction period ($h_r = 30$ years). However, the increase in the aggregated life expectancy is now compensated for by the higher mortality of cohorts born during the reverse cohort effect, which have a higher level of deprivation. Firstly, the period life expectancy progressively decreases up to time t=40, due to the 'reverse' cohort effect. At the end of the reduction period ($t = t_r + h_r$), the more deprived individuals born in $[0, h_b]$ are in the age class 50-70, and the period life expectancy decreases due to the progressive increase in deprivation level of older individuals.

Due to this compensation effect, the period life expectancy is lower in Scenario 2 than in Scenario 1a (Figure 14a). When the CVD mortality reduction attains $\alpha = 20\%$, the male period life expectancy at age 25 is respectively 54.6, 54.5, 54.4 in Scenario 2 with $\beta = 20\%, 40\%$ and 60%, in comparison with 54.8 where there are no changes of composition in the population (Scenario 1a). Depending on the value of β, this corresponds to a compensation of 32%, 58% and 81% of the increase in the period life expectancy caused by the CVD mortality reduction. When individuals born during the reverse cohort effect grow older, the cause-of-death mortality reduction can even be counterbalanced by the cohort effect. This is the case when $\beta = 60\%$[18]: the increase in life expectancy due to the cause specific reduction is compensated for when the oldest individuals (born at $t = 0$) in the more deprived cohorts attain age 76.

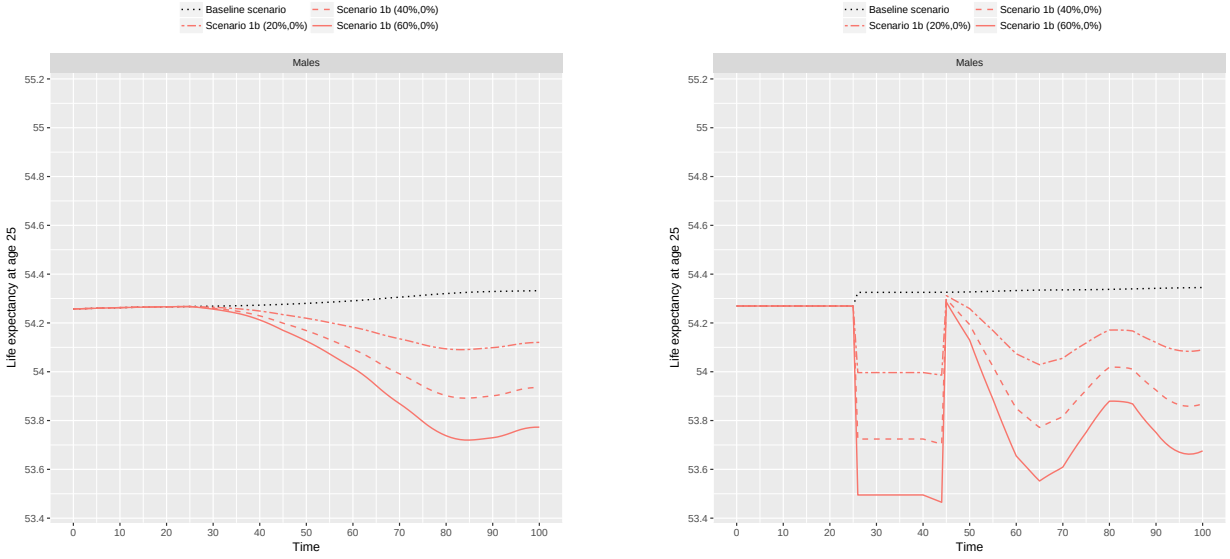

(a) Period life expectancy

(b) Cohort life expectancy

Figure 13: Aggregated male life expectancy: reverse cohort effect (scenario 1b)

The other causes considered (Figure 14b) are numbered from 1 to 4 per order of importance: neoplasms (1), CVD (2), respiratory diseases (3) and external causes (4), with parameters $\alpha = 20\%$ and $\beta = 60\%$. All cause-of-death mortality reductions, except neoplasms, are eventually compensated for by the cohort effect. Naturally, the direction and magnitude of the impact of the cause reductions depend on the cause of death that is reduced, since different causes do not impact all age groups and socioeconomic categories in

[18]Cohorts born during the period $[0, 20[$ composed of 63% of individuals in Subpopulation 5.

the same way. In particular, for causes 3 and 4, which are less important, the aggregated period life expectancy even decreases over time due to the compensation effect, and that could be incorrectly interpreted as an increase of mortality rates.
Similar conclusions hold as well for the aggregated cohort life expectancy in term of cause-specific mortality reduction compensation (Figure 15). Nevertheless, as in Scenario 1b, the impact of the reverse cohort effect is more clear-cut when looking at the cohort index. Figure 15b shows that for all causes of death, the cohort life expectancy at 25 of the cohorts more deprived (corresponding to the cohort life expectancy from time $t = 25$ to $t = 25 + h_b = 45$) is lower than in the baseline scenario. This means that the increase in deprivation of these cohorts has more impact than the cause-of-death mortality reduction.

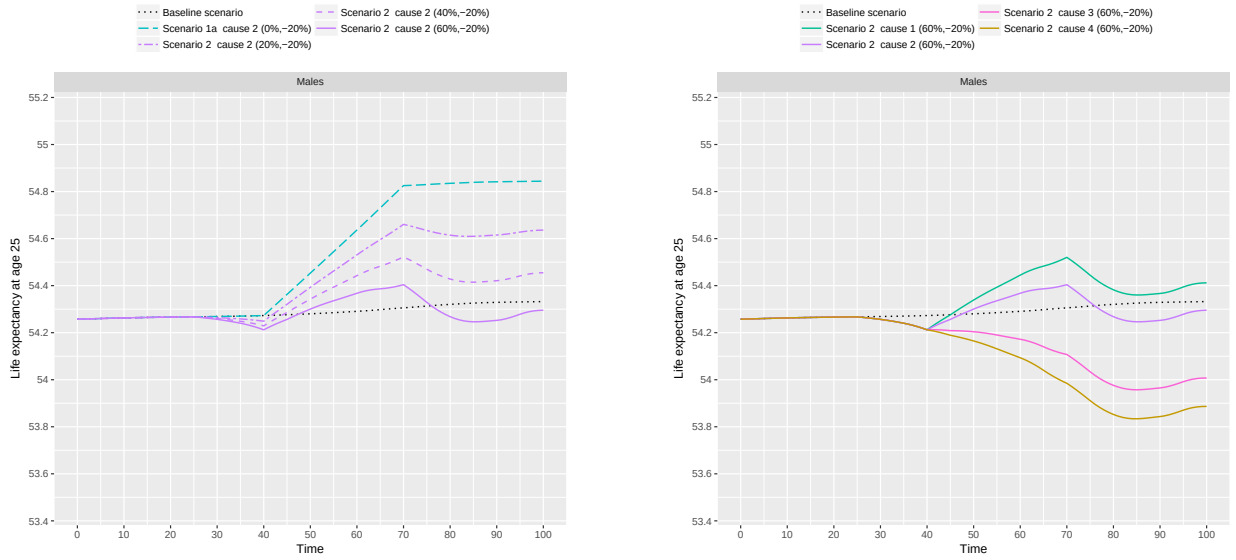

(a) Cardiovascular diseases (b) All causes

Figure 14: Aggregated male period life expectancy over time (scenario 2)

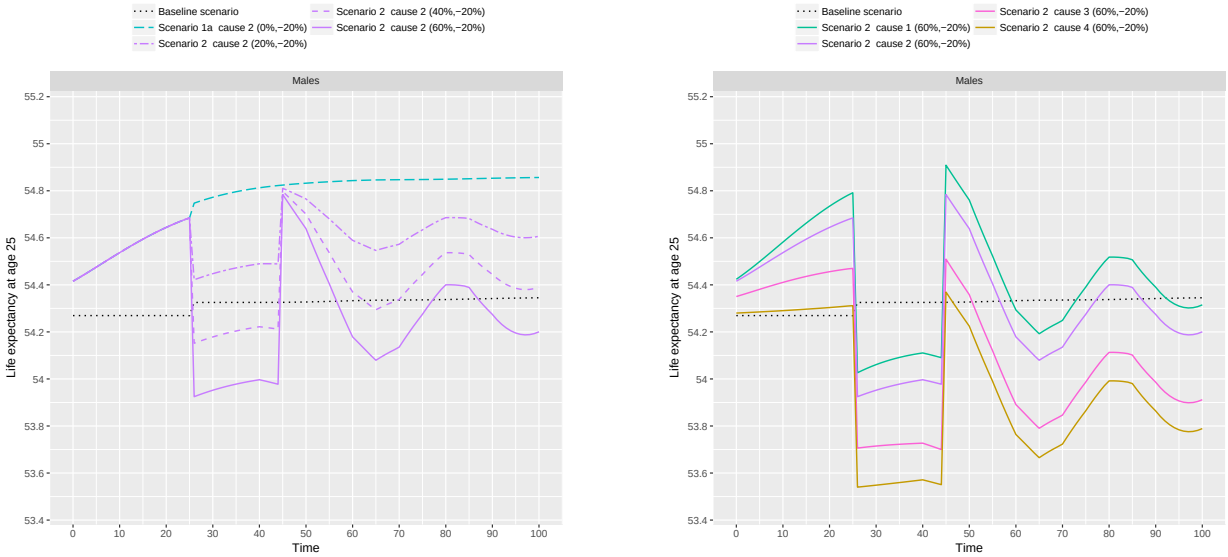

(a) Cardiovascular diseases (b) All causes

Figure 15: Aggregated male cohort life expectancy over time (scenario 2)

Discussion The demographic scenarios presented in this section illustrate the complexity induced by the presence of heterogeneity. Figures 14 and 15 show that when the socioeconomic composition of the population changes over time, the sole study of aggregated period indexes can lead to misinterpretations of mortality trends. For instance, a "true" mortality reduction driven by a cause-of-death reduction could be minimized, or even not accounted for, due to structural changes in the population composition.

It is also important to note that the demographic changes in Scenarios 1a and 1b (cause-of-death mortality reduction and reverse cohort effect) operate on very different timescales, which add to the complexity of understanding aggregated indicators. In Scenario 2, the change of composition due to the reverse cohort effect has a delayed impact on the aggregated mortality, and compensates for the increase in life expectancy because individuals in the more deprived cohorts (born during the period $[0, h_b]$) are old enough when the progressive cause-of-death mortality reduction starts at time t_r. When the mortality reduction starts at an earlier time t_r, the life expectancy first increases (more deprived individuals are too young to weight in the period life expectancy), but then starts to decrease faster at the end of the mortality reduction period (after time $t_r + h_r$), as individuals in more deprived cohorts grow older and have more weight in the aggregated period life expectancy. On the other hand, when the mortality reduction starts at a later time t_r, the adverse mortality of individuals born during the reverse cohort effect compensates for the mortality reduction earlier and more strongly.

In order to compare the different demographic rates, the population composition is modified using fertility rates in Scenarios 1b and 2. However, compositional changes could be caused by other underlying mechanisms such as internal or external migrations. Recent changes in internal migration patterns in England suggest that these mechanisms could generate compositional changes comparable in order of magnitude to those presented in this section, although these changes might not be as stable over time as in Scenario 1a. Thus, including internal migrations should be an important part of a further work. However, the lack of data might remain an important challenge to overcome.

Finally, the cause-of-death independence assumption could be relaxed by using a model allowing for dependence between causes of death such as that proposed in Dimitrova et al. (2013) or Alai et al. (2015), or Girosi and King (2008) in a Bayesian framework. It is worth noting that under our assumption of independence between causes of death, a decrease in CVD mortality decreases the life expectancy gap between the least and the most deprived subpopulations, while Alai et al. (2017), using the model proposed in Alai et al. (2015), found that the cause elimination of CVD would actually have increased the life expectancy gap, under the mortality conditions of most years over the period 1981-2007. An increase in the mortality gap between the most and least deprived subpopulations would actually magnify the effect of composition changes, and one could expect that a model allowing for dependence would strengthen the previous results.

5 Concluding Remarks

We have illustrated in this paper the complexity of understanding drivers of the aggregated mortality in the presence of heterogeneity. The data analysis and numerical applications presented reveal the complex interactions between population dynamics and mortality indicators. In the context of increasing differences in mortality between different socioeconomic subgroups, changes in population composition have more impact on the aggregate population mortality. At the same time, significant variations of deprivation levels have occurred across age groups and over time. Those notable changes in the population composition make studying the effect of composition changes even more complicated.

Numerical results presented in Section 4.1 show that favorable changes in population composition since 1981 might have contributed positively to the increase in aggregated life expectancy, while the model shows that based on the 2015 population, composition changes might offset future mortality improvements to a certain extent.

Furthermore, the reduction of a cause of death may not necessarily result in an improvement of aggregate mortality rates or life expectancy, if the composition of the population changes at the same time. In particular, a 'reverse' cohort effect, or any changes in the population composition, could compensate for a cause-of-death reduction. In this case, the effect of public health policies could be misinterpreted if only aggregated data are studied. This raises the question of the assessment of mortality reduction targets set by national or international organization in the presence of heterogeneity. Indeed, it seems rather difficult, by only looking at aggregated indicators, to determine if a target is not met due to the failure of a public health policy or a change in population composition.

The results also stress the importance of studying not only mortality rates at older ages but also the whole population dynamics in the presence of heterogeneity, as mortality models which may not be able to capture population composition changes.

Depending on the nature of demographic changes and on the timing at which they impact the aggregate mortality, different changes are captured by different types of indicators, i.e. period or cohort indicators. In particular, we showed that composition changes, which can have a delayed effect on mortality, seem to be better captured by cohort indicators. Obviously, cohort indicators require to forecast future mortality rates in order to be computed. However, due to these delayed effects, taking into account the population composition and age structure gives insight into how future composition changes might impact mortality rates.

Finally, the population dynamics framework is very flexible. The model considered in this paper allows us to reproduce composition changes and capture non-trivial effects of the heterogeneous population dynamics. However, the framework could actually be extended without difficulty to the broader scope of stochastic rates, depending for instance on a random environment. Further work could also investigate the use of stochastic individual-based models.

In the numerical applications presented in Section 4.2, composition changes were modeled by differences in fertility rates, in order to compare these variations with a cause-of-death

mortality reduction. Nevertheless, modification of the population composition could be extended to other underlying mechanisms. Thus, a more realistic modeling procedure could integrate internal migrations among the subpopulations, as well as external migrations. This constitutes a challenge due to data availability, but the population dynamics framework can operate as a tool for experimenting and simulating different scenarios. Another perspective would be to consider dependence between causes of death in the modeling, along with the study of consistency between subnational and national mortality forecasts (Shang and Hyndman (2017), Shang and Haberman (2017)).
To conclude, population dynamics theory is a promising and complementary field of research when modeling mortality rates in the presence of heterogeneity. The richness of available models should allow them to be used as simulation and validation tools. Additionally, they can capture dynamically effects of a different nature with respect to classical mortality modeling, such as composition changes.

Acknowledgements

The authors benefited from the financial support of the "Germaine de Staël" program *Modélisation des causes de décès dans la dynamique des populations* (Gds 2014-14), and the ANR project *Dynamic models for longevity with lifestyle adjustments* (ANR-13-BS01-0011). The authors also thank Madhavi Bejekal and Andres Villegas for their great help for obtaining the first dataset and their explanations.

References

Alai, D., Arnold, S., Bajekal, M., and Villegas, A. (2017). Causal mortality by socioeconomic circumstances: A model to assess the impact of policy options on inequalities in life expectancy. In *Conference proceedings of the Society of Actuaries 2017 Living to 100 Symposium*.

Alai, D., Arnold(-Gaille), S., and Sherris, M. (2015). Modelling Cause-of-Death Mortality and the Impact of Cause-Elimination. *Annals of Actuarial Science*, 9(1):167–186.

Bajekal, M. (2005). Healthy life expectancy by area deprivation: magnitude and trends in England, 1994-1999. *Health Statistics Quarterly*, 25:18.

Bajekal, M., Scholes, S., O'Flaherty, M., Raine, R., Norman, P., and Capewell, S. (2013a). Implications of using a fixed IMD quintile allocation for small areas in England from 1981 to 2007. *PLoS One*, 8(3).

Bajekal, M., Scholes, S., O'Flaherty, M., Raine, R., Norman, P., and Capewell, S. (2013b). Unequal trends in coronary heart disease mortality by socioeconomic circumstances, England 1982–2006: an analytical study. *PLoS One*, 8(3):e59608.

Boumezoued, A., Labit Hardy, H., El Karoui, N., and Arnold, S. (2018). Cause-of-death mortality: What can be learned from population dynamics? *Insurance: Mathematics and Economics*, 78:301 – 315. Longevity risk and capital markets: The 201516 update.

Cairns, A., Kallestrup-Lamb, M., Rosenskjold, C., Blake, D., and Dowd, K. (2016). Modelling socio-economic differences in the mortality of Danish males using a new affluence index. Working paper.

Chiang, C. (1968). Introduction to stochastic processes in biostatistics. *John Wiley and Sons, New York*.

Department for Communities and Local Government (2015). The English Indices of Deprivation 2015 - Statistical release. Technical report, Department for Communities and Local Government.

Department of Health (2003). Tackling Health Inequalities: A Programme for Action. Technical report, Department of Health.

Diez Roux, A. V. and Mair, C. (2010). Neighborhoods and health. *Annals of the New York Academy of Sciences*, 1186(1):125–145.

Dimitrova, D., Haberman, S., and Kaishev, V. (2013). Dependent competing risks: Cause elimination and its impact on survival. *Insurance: Mathematics and Economics*, 53(2):464–477.

El Karoui, N., Hadji, K., and Kaakai, S. (2018). Inextricable complexity of two centuries of worlwide demographic transition: a fascinating modeling challenge. *Hal-01745901*.

Elo, I. T. (2009). Social class differentials in health and mortality: Patterns and explanations in comparative perspective. *Annual Review of Sociology*, 35:553–572.

Girosi, F. and King, G. (2008). *Demographic Forecasting*. Princeton University Press, Princeton.

Guildea, Z., Fone, D., Dunstan, F., Sibert, J., and Cartlidge, P. (2001). Social deprivation and the causes of stillbirth and infant mortality. *Archives of Disease in Childhood*, 84(4):307–310.

Haberman, S., Kaishev, V., Millossovich, P., and Villegas, A. (2014). Longevity Basis Risk A methodology for assessing basis risk. Technical report, Institute and Faculty of Actuaries (IFA), Life and Longevity Markets Association (LLMA).

Hautphenne, S. and Latouche, G. (2012). The Markovian binary tree applied to demography. *Journal of Mathematical Biology*, 64(7):1109–1135.

Iannelli, M., Martcheva, M., and Milner, F. A. (2005). *Gender-structured Population Modeling: Mathematical methods, Numerics, and Simulations*, volume 31. SIAM.

Inaba, H. (2017). *Age-Structured Population Dynamics in Demography and Epidemiology*. Springer Singapore.

Jarner, S. F. and Kryger, E. M. (2011). Modelling adult mortality in small populations: The SAINT model. *ASTIN Bulletin: The Journal of the IAA*, 41(2):377–418.

Jasilionis, D., Andreev, E. M., Kharkova, T. L., and Ward Kingkade, W. (2011). Change in marital status structure as an obstacle for health improvement: evidence from six developed countries. *The European Journal of Public Health*, 22(4):602–604.

Keyfitz, N. and Caswell, H. (2005). *Applied mathematical demography*, volume 47. Springer.

Kontopantelis, E., Mamas, M. A., van Marwijk, H., Buchan, I., Ryan, A. M., and Doran, T. (2018). Increasing socioeconomic gap between the young and old: temporal trends in health and overall deprivation in england by age, sex, urbanity and ethnicity, 2004–2015. *J Epidemiol Community Health*, pages jech–2017.

Labit Hardy, H. (2016). *Impacts of cause-of-death mortality changes: A population dynamic approach*. PhD thesis, Université de Lausanne.

Li, J. K. K., Tickle, L., and Tan, C. I. (2017). Assessing basis risk for longevity transactions - phase 2. *Macquarie University, Institute and Faculty of Actuaries (IFoA), and Life and Longevity Markets Association (LLMA)*.

Li, J. S.-H., Zhou, R., and Hardy, M. (2015). A step-by-step guide to building two-population stochastic mortality models. *Insurance: Mathematics and Economics*, 63:121 – 134. Special Issue: Longevity Nine - the Ninth International Longevity Risk and Capital Markets Solutions Conference.

Lu, J., Wong, W., and Bajekal, M. (2014). Mortality improvement by socio-economic circumstances in England (1982 to 2006). *British Actuarial Journal*, 19(01):1–35.

Ludkovski, M., Risk, J., and Zail, H. (2016). Gaussian process models for mortality rates and improvement factors. *arXiv:1608.08291*.

Mackenbach, J. P., Kunst, A. E., Cavelaars, A. E., Groenhof, F., and Geurts, J. J. (1997). Socioeconomic inequalities in morbidity and mortality in western Europe. *The Lancet*, 349(9066):1655 – 1659.

Marmot, M., Stansfeld, S., Patel, C., North, F., Head, J., White, I., Brunner, E., Feeney, A., and Smith, G. D. (1991). Health inequalities among British civil servants: the Whitehall II study. *The Lancet*, 337(8754):1387 – 1393. Originally published as Volume 1, Issue 8754.

McKendrick, A. (1926). Application of mathematics to medical problems. *Proc. Edin. Math. Soc.*, 54:98–130.

Meyricke, R. and Sherris, M. (2013). The determinants of mortality heterogeneity and implications for pricing annuities. *Insurance: Mathematics and Economics*, 53(2):379–387.

Nandi, A. and Kawachi, I. (2011). Neighborhood effects on mortality. In *International Handbook of Adult Mortality*, pages 413–439. Springer.

National Research Council (2011). *Explaining divergent levels of longevity in high-income countries*. National Academies Press.

Noble, M., Mclennan, D., Wilkinson, K., Whitworth, A., Barnes, H., and Dibben, C. (2007). The English indices of Deprivation 2007. Technical report, Department of Communities and Local Government.

Norman, P. and Darlington-Pollock, F. (2017). The Changing Geography of Deprivation in Great Britain: Exploiting Small Area Census Data, 1971 to 2011. In Stillwell, J., editor, *The Routledge Handbook of Census Resources, Methods and Applications Unlocking the UK 2011 Census*, pages 404–420. Routledge.

Oakley, L., Maconochie, N., Doyle, P., Dattani, N., and Moser, K. (2009). Multivariate analysis of infant death in England and Wales in 2005-06, with focus on socio-economic status and deprivation. *Health Statistics Quarterly*, 42(1):22–39.

Office for National Statistics (2012). *2011 Census: Population and Household Estimates for Small Areas in England and Wales, March 2011*. Office for National Statistics.

Office for National Statistics (2015a). Live births, stillbirths, and the intensity of childbearing measured by the total fertility rate. Access date: May 2016.

Office for National Statistics (2015b). Trend in life expectancy at birth and at age 65 by socio-economic position based on the National Statistics Socio-economic Classification, England and Wales: 1982-1986 to 2007-2011. Technical report, Office for National Statistics.

Office for National Statistics (2018a). How do the post-World War baby boom generations compare? Technical report, Office for National Statistics.

Office for National Statistics (2018b). Living longer: how our population is changing and why it matters. Technical report, Office for National Statistics.

Pamuk, E. R. (1985). Social Class Inequality in Mortality from 1921 to 1972 in England and Wales. *Population Studies*, 39(1):17–31. PMID: 11611750.

Pelovska, G. and Iannelli, M. (2006). Numerical methods for the Lotka-Mckendrick's equation. *Journal of Computational and Applied Mathematics*, 197(2):534–557.

Shang, H. L. and Haberman, S. (2017). Grouped multivariate and functional time series forecasting: An application to annuity pricing. *Insurance: Mathematics and Economics*.

Shang, H. L. and Hyndman, R. J. (2017). Grouped functional time series forecasting: An application to age-specific mortality rates. *Journal of Computational and Graphical Statistics*, 26(2):330–343.

Shkolnikov, V. M., Andreev, E. M., Jasilionis, D., Leinsalu, M., Antonova, O. I., and McKee, M. (2006). The changing relation between education and life expectancy in central and eastern europe in the 1990s. *Journal of Epidemiology and Community Health*, 60(10):875–881.

The Human Mortality Database (2016). University of California, Berkeley (USA), and Max Planck Institute for Demographic Research (Germany). English data, access date: February 2016.

Villegas, A. M. (2015). *Mortality: Modelling, Socio-Economic Differences and Basis Risk*. PhD thesis, Cass Business School.

Villegas, A. M. and Haberman, S. (2014). On the modeling and forecasting of socioeconomic mortality differentials: An application to deprivation and mortality in England. *North American Actuarial Journal*, 18(1):168–193.

Villermé, L. (1830). De la mortalité dans les divers quartiers de la ville de Paris, et des causes qui la rendent très différentes dans plusieurs d'entre eux, ainsi que dans les divers quartiers de beaucoup de grandes villes. *Annales d'hygiène publique et de médecine légale*, 3:294–321.

Von Foerster, H. (1959). *The Kinetics of Cellular Proliferation*. Grune & Stratton.

Webb, G. F. (1985). *Theory of nonlinear age-dependent population dynamics*. CRC Press.

World Health Organization (2013). Global action plan for the prevention and control of noncommunicable diseases 2013-2020. Technical report, World Health Organization.

Appendix A IMD over time

The IMD is computed at fixed times, year 2007 and year 2015, and applied to larger time periods, see Figure 16. Therefore, the socioeconomic evolution of living areas over the reporting periods is not taken into account. However, the aggregation of small living areas into deprivation quintiles might reduce changes over reasonable periods of time. For the 1981-2006 period, previous studies have shown that the majority of small areas have stayed in the same deprivation quintile (se e.g. Bajekal et al. (2013a), Appendix D of Lu et al. (2014) or Norman and Darlington-Pollock (2017) for the 1970-2011 period).

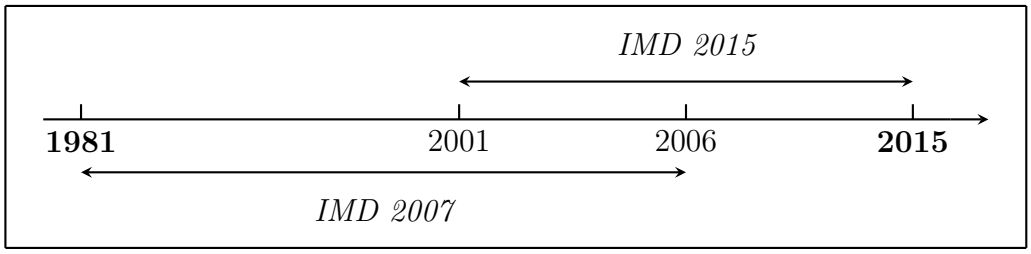

Figure 16: IMD2007-IMD2015

We have also compared data over the 2001-2006 period, computed with the IMD 2007 in the one hand (dataset 1) and with the IMD 2015 in the other hand (dataset 2). For the overlapping period 2001-2006, over the five quintiles, the relative difference in life expectancy at age 25, *respectively* at age 65, using IMD 2007 or IMD 2015 is less than $0,27\%$, *resp.* $0,78\%$, for males and less than $0,18\%$, *resp.* $0,46\%$, for females.

Appendix B Miscellaneous information on data

B.1 Fixed cohorts

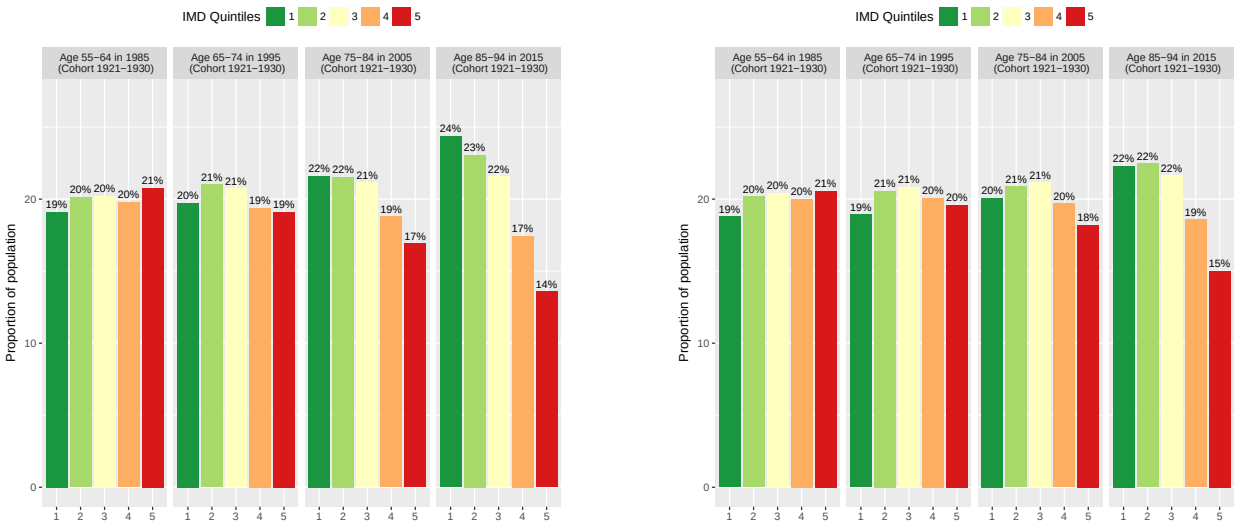

(a) Males (b) Females

Figure 17: Proportion of individuals by IMD quintile for cohort 1921-1930 (1985, 1995, 2005, 2015)

B.2 Mortality rates

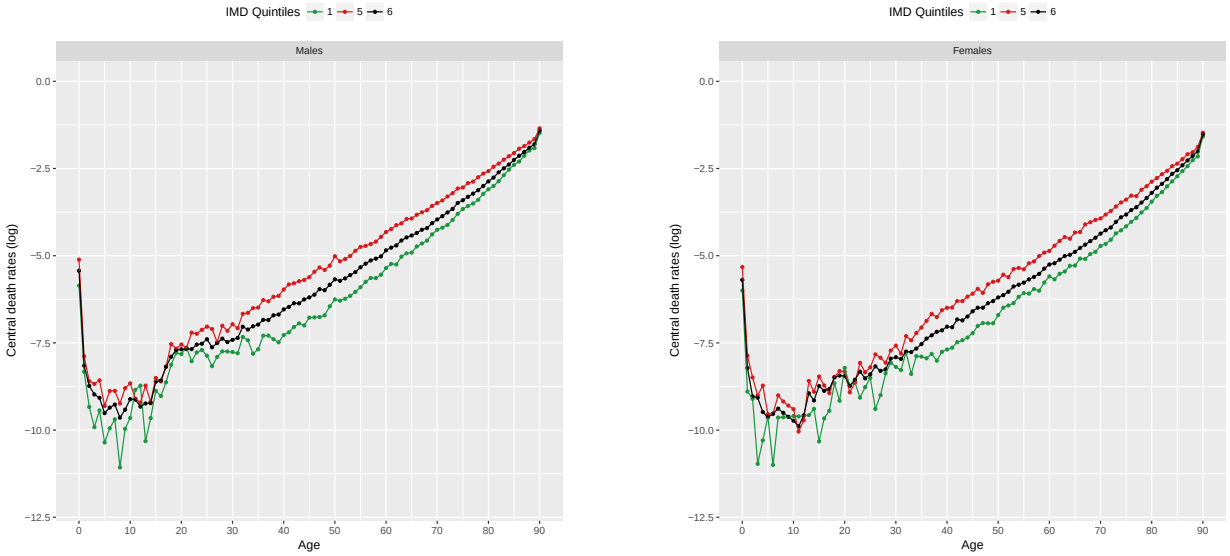

(a) Males (b) Females

Figure 18: Central death rates per single year of age and IMD quintile in 2015

B.3 Central death rates

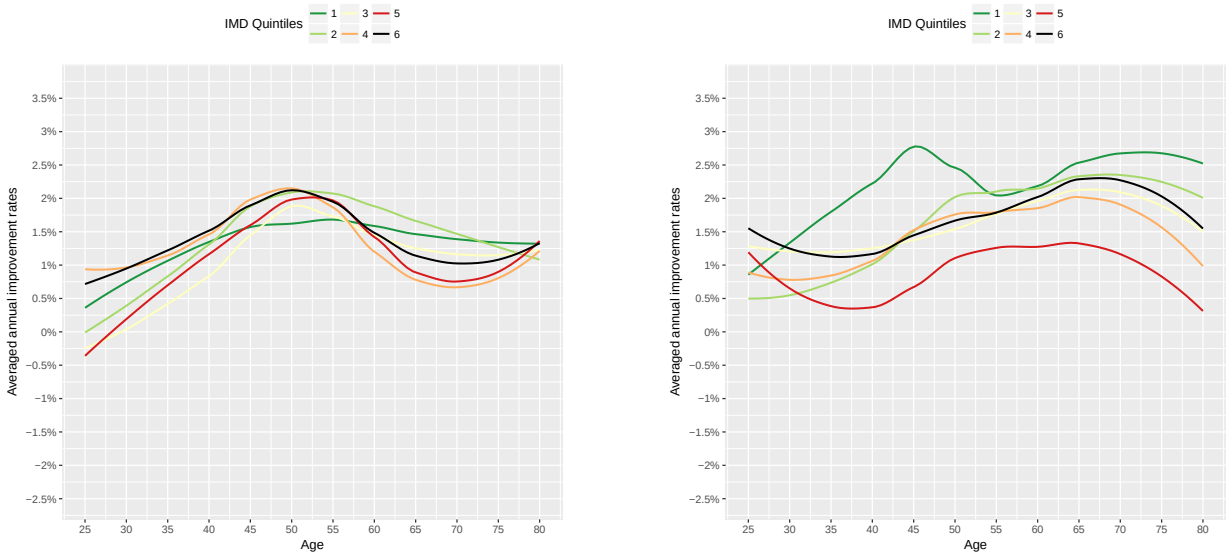

(a) 1981-1995 (b) 2001-2015

Figure 19: Average annual rates of improvement in mortality, females

B.4 Causes of death

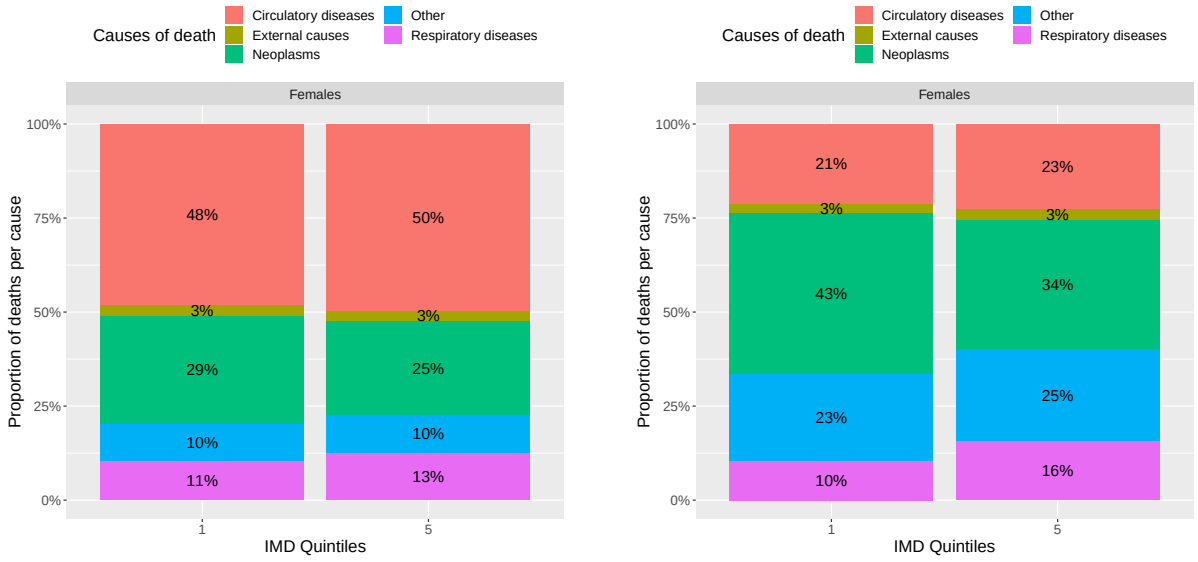

(a) 1981 (b) 2015

Figure 20: Females deaths per cause and IMD quintile for ages 25-85

Appendix C Numerical implementation

The general model is implemented in C++ by discretization of the transport partial differential equation (1), using a first order implicit Euler scheme. More details on the convergence and stability of the scheme, as well as other numerical methods, can be found in the review of Pelovska and Iannelli (2006).

In the different applications presented in Section 4, the parameters of the model (mortality, fertility rates and initial age pyramids) are estimated from the data presented in Section 2. The inputs and outputs of the model are processed using R, and interfaced with the C++ code using the package Rcpp. When only central death rates by 5-year age classes are given, mortality rates are estimated based on the fitting procedure described in Appendix D. Furthermore, individuals in each IMD quintile of age above 85 are grouped in the age class "85 and older" in dataset 1[19]. To overcome this difficulty, we assume that individuals are distibuted in age classes until age 110 as in the UK population[20]. This assumption is consistent with the observation that mortality rates in all IMD quintiles converge at old ages.

Appendix D Fitting procedure of mortality rates

In this paragraph, we consider the mortality of individuals of gender ϵ in a given IMD quintile j. For simplicity of notation, we omit these variables when there is no ambiguity. In both datasets, deaths by causes are given for each calendar year by 5-year age classes (with the exception of the age class 0-5 divided in two classes, 0-1 and 1-5). Central death

[19] 90 and older in Dataset 2.

[20] The English age pyramid after age 85 is provided by the Human Mortality Database (The Human Mortality Database (2016)).

rates at age a and year t for 5-year age classes can been estimated by ${}_5\hat{m}(a,t) = \frac{{}_5D(a,t)}{{}_5\hat{E}(a,t)}$; where ${}_5D(a,t)$ is the number of individuals who died during year t (in $[t, t+1[$) at an age in $[a, a+5[$, and where ${}_5\hat{E}(a,t)$ is the estimated exposure. Recall that the real exposure ${}_5E(a,t)$ is the cumulative time lived during year t by individuals in the age class[21].
In our model, we need to estimate the force of mortality $\mu(a,t)$ which is linked to the theoretical death rate by the following formula:

$$ {}_5m(a,t) = \int_t^{t+1} \int_a^{a+5} \mu(x,s) \frac{g(x,s)}{\int_t^{t+1} \int_a^{a+5} g(u,h)\mathrm{d}u\mathrm{d}h} \mathrm{d}x\mathrm{d}s \tag{14} $$

Equation (14) can be interpreted as follow: the central death rate is the average force of mortality on $[t, t+1[\times[x, x+5[$, weighted against the population distribution on this interval.
In the sequel, we make the assumption that the force of mortality is constant over each 1 year period, so that for all calendar years t, $\mu(a, t+s) = \mu(a,t) \quad \forall s \in [0,1[$. In this case, Equation (14) can be rewritten as:

$$ {}_5m(a,t) = \int_a^{a+5} \mu(x,t) \frac{\int_t^{t+1} g(x,s)ds}{\int_a^{a+5} (\int_t^{t+1} g(u,s)du)ds} \mathrm{d}x $$

When data is structured by single year of age, the force of mortality is usually also assumed to stay constant over each age class, so that $\mu(x,t) = {}_1m(a,t)$ for $a \leqslant x < a+1$. However, this assumption seems quite unrealistic when data is aggregated over 5 year age classes. The next simplest parametric assumption is to assume that the force of mortality is piecewise linear in age over the age classes:

$$ \mu(x,s) = \alpha(a,t)x + \beta(a,t) \quad \forall (x,s) \in [a, a+5[\times[t, t+1[. \tag{15} $$

When information on the population by single years of age is available, the distribution of the population within the age class can be approximated by a discrete distribution defined for $0 \leqslant k \leqslant 4$ by:

$$ \frac{\int_t^{t+1} g(x,s)ds}{\int_a^{a+5} \left(\int_t^{t+1} g(u,s)ds\right) \mathrm{d}u} = \hat{E}_k, \quad \forall x \in [a+k, a+k+1[, $$

where $\hat{E}_k$ is the estimated proportion of individuals of age in $[a+k, a+k+1[$ in the the age class. By replacing $\mu(a,t)$ and $g(x,s)$ in (14) with the new assumptions, we obtain that Equation (15) should be a line passing through ${}_5m(x,t)$ at the mean age of individuals in the age class. Therefore, an inductive procedure can be defined in order to fit the force of mortality for year t:

(i) *Initialization:* Choose $\mu(0,t)$.

(ii) *Induction:* Assume that the mortality rate has been fitted until the ith age class $[a_i, a_{i+1}[$. The mortality rate on the next age class $[a_{i+1}, a_{i+2}[$ is the line passing through $\mu(a_{i+1}, t)^-$ at a_{i+1} and ${}_5m(x_{i+1}, t)$ at $\bar{x}_{i+1}$.

[21] An individual attaining age a at time $t+s$ and who died at time $t+h+s < t+1$ will have weight h in the exposure.

(iii) Reiterate the second step on the next age class.

The main advantage of the piecewise linear approximation is to be consistent with the theoretical definition of the aggregated and specific central death rates in our heterogeneous population model. However, the degree of liberty in the choice of the initial point $\mu(0,t)$ is a drawback of the method, and the fitting is not guaranteed to obtain positive death rates. In the numerical applications the initial point $\mu(0,t)$ is found by an optimization procedure. A similar fitting approach has been proposed by Hautphenne and Latouche (2012), with possible discontinuities in the death rates. See also Villegas and Haberman (2014) for an alternative method.